Article

Cell Host & Microbe

Fusion Stage of HIV-1 Entry Depends on Virus-Induced Cell Surface Exposure of Phosphatidylserine

Graphical Abstract

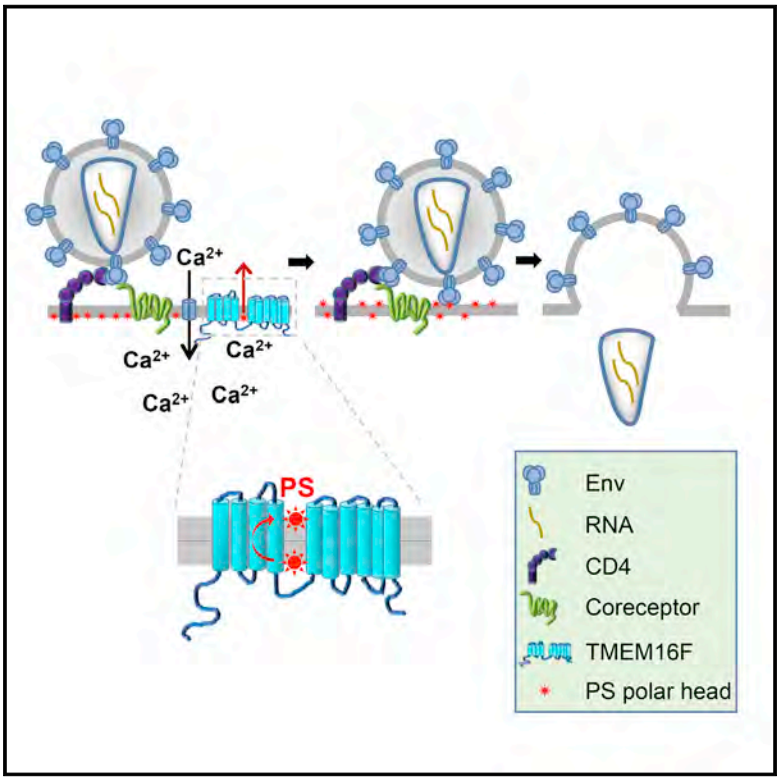

Authors

Elena Zaitseva, Eugene Zaitsev, Kamran Melikov, ..., Leonid B. Margolis, Gregory B. Melikyan, Leonid V. Chernomordik

Correspondence

chernoml@mail.nih.gov

In Brief

Zaitseva et al. show that HIV binding to target cells induces signaling that leads to exposure of phosphatidylserine on the cell surface. Interaction between the viral envelope glycoprotein and phosphatidylserine facilitates receptor-dependent merger of viral and cell membranes and infection. Phosphatidylserine dependence may focus infection on cells of certain activation status.

Highlights

- HIV-cell binding triggers phosphatidylserine (PS) exposure at the cell surface
- PS exposure depends on gp120-coreceptor interactions, Ca^{2+} signaling, and TMEM16F
- Suppression of PS exposure inhibits Env restructuring, viral fusion, and infection
- PS signaling, a hallmark of activation, facilitates HIV entry

Zaitseva et al., 2017, Cell Host & Microbe 22, 99–110
July 12, 2017 Published by Elsevier Inc.
http://dx.doi.org/10.1016/j.chom.2017.06.012

Cell Host & Microbe
Article

Fusion Stage of HIV-1 Entry Depends on Virus-Induced Cell Surface Exposure of Phosphatidylserine

Elena Zaitseva,[1] Eugene Zaitsev,[1] Kamran Melikov,[1] Anush Arakelyan,[2] Mariana Marin,[3] Rafael Villasmil,[4] Leonid B. Margolis,[2] Gregory B. Melikyan,[3] and Leonid V. Chernomordik[1,5,*]
[1]Section on Membrane Biology, Eunice Kennedy Shriver National Institute of Child Health and Human Development, National Institutes of Health, Bethesda, MD, USA
[2]Section on Intercellular Interactions, Eunice Kennedy Shriver National Institute of Child Health and Human Development, National Institutes of Health, Bethesda, MD, USA
[3]Department of Pediatrics, Emory University School of Medicine, Atlanta, GA, USA
[4]Flow Cytometry Core, National Eye Institute, National Institutes of Health, Bethesda, MD, USA
[5]Lead Contact
*Correspondence: chernoml@mail.nih.gov
http://dx.doi.org/10.1016/j.chom.2017.06.012

SUMMARY

HIV-1 entry into host cells starts with interactions between the viral envelope glycoprotein (Env) and cellular CD4 receptors and coreceptors. Previous work has suggested that efficient HIV entry also depends on intracellular signaling, but this remains controversial. Here we report that formation of the pre-fusion Env-CD4-coreceptor complexes triggers non-apoptotic cell surface exposure of the membrane lipid phosphatidylserine (PS). HIV-1-induced PS redistribution depends on Ca^{2+} signaling triggered by Env-coreceptor interactions and involves the lipid scramblase TMEM16F. Externalized PS strongly promotes Env-mediated membrane fusion and HIV-1 infection. Blocking externalized PS or suppressing TMEM16F inhibited Env-mediated fusion. Exogenously added PS promoted fusion, with fusion dependence on PS being especially strong for cells with low surface density of coreceptors. These findings suggest that cell-surface PS acts as an important cofactor that promotes the fusogenic restructuring of pre-fusion complexes and likely focuses the infection on cells conducive to PS signaling.

INTRODUCTION

Human immunodeficiency virus 1 (HIV-1), the causative agent of AIDS, delivers its RNA into cells by fusing the viral envelope with the cell membrane. This fusion process is mediated by viral envelope glycoprotein Env, a trimer of heterodimers consisting of gp120 and gp41 subunits. Fusion is initiated by gp120 interactions with CD4 and one of the two coreceptors CCR5 and CXCR4 at the surfaces of the target cells (Doms and Peiper, 1997; Melikyan, 2008). A number of studies, and especially studies of resting primary cells, have suggested that an efficient Env-mediated fusion and infection also depends on intracellular signaling. Specifically, Ca^{2+} signaling is triggered by engagement of the coreceptors with gp120 (Davis et al., 1997; Harmon et al., 2010; Harmon and Ratner, 2008; Melar et al., 2007; Wilen et al., 2012; Wu and Yoder, 2009). However, the role of signaling in HIV-1 fusion/infection remains controversial and appears to be cell-type- and activation status-dependent (reviewed in Wilen et al., 2012).

A sustained rise in intracellular Ca^{2+} triggers a transient redistribution of phosphatidylserine (PS) from the PS-enriched inner leaflet to the normally PS-free outer leaflet of the plasma membrane (Suzuki et al., 2010). The "scrambling" of the distribution of PS between the membrane leaflets is mediated by a member of the family of *Ca*$^{2+}$-activated *c*hloride *c*hannels and scramblases (CaCCs), transmembrane protein 16F (TMEM16F, also known as anoctamin 6 HGNC:25240) (Segawa et al., 2011; Suzuki et al., 2010).

In this work, we report that HIV-1 binding to its receptors induces non-apoptotic exposure of PS at the surface of the target cell and that externalized PS strongly promotes Env-mediated membrane fusion and HIV-1 infection. Specific interactions between the gp120 subunit of Env of cell-surface-bound virions and coreceptors triggered Ca^{2+} signaling-dependent TMEM16F-mediated PS externalization in the plasma membrane. Blocking externalized PS with PS-binding proteins or suppressing TMEM16F function inhibited Env-mediated fusion at a stage preceding membrane merger. Exogenous PS added to the plasma membrane promoted fusion, and the extent of this promotion increased for the target cells with lower levels of coreceptor expression and upon reduction of the number of fusion-competent Envs. The uncovered link between HIV-1 infection and PS externalization identifies a bi-directional signaling pathway in which the classic outside-in signaling through GPCR-coreceptor triggers, via intracellular Ca^{2+} rise, inside-out PS externalization signaling mediated by TMEM16F. In the context of HIV entry, our findings suggest that within the diverse populations of target cells HIV-1 infects the CD4- and coreceptor-expressing cells that mount the signaling responses

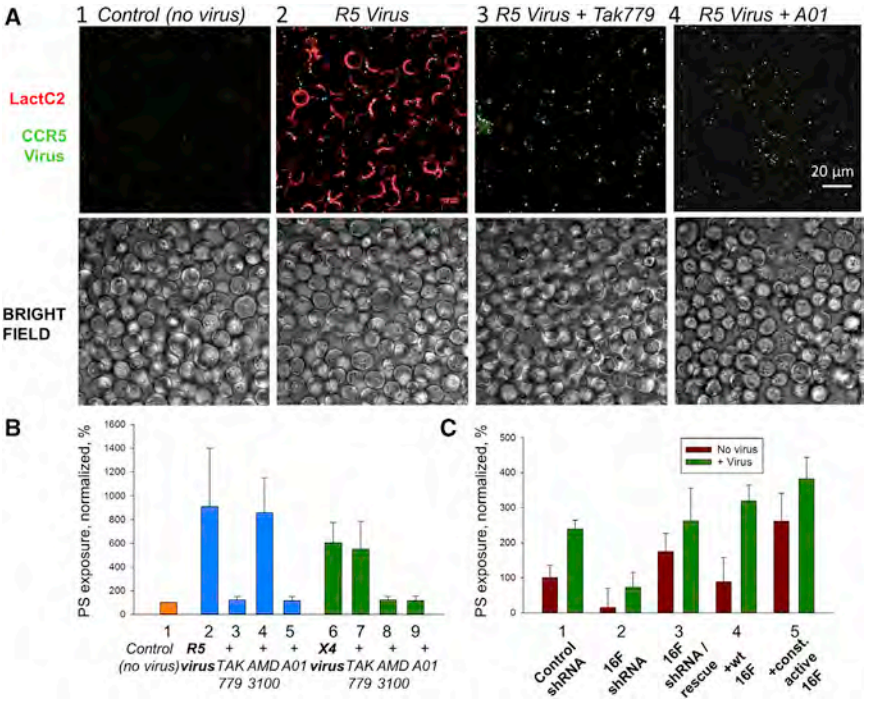

Figure 1. Binding of HIV-1 Pseudovirus to the Target Cell Induces Coreceptor-Dependent and TMEM16F-Mediated PS Exposure at the Cell Surface

(A) JkT-CCR5 cells were incubated with GaG-Clover R5-tropic pseudovirus (JR-FL) (2, 3, 4) (38 ng p24/ml) or mock solution (1) at 22°C for 15 min; then, Ruby-LactC2 was added and 45 min later unbound viruses were removed and the cells were imaged. 1 μM CCR5 antagonist TAK-779 (3) and 60 μM TMEM16-inhibitor A01 (4) were added as described in STAR Methods. Top images show LactC2 in red and virus in green. Bottom images are bright field.

(B) PS exposure at the surface of JkT-CCR5 cells for R5-tropic (JR-FL) (38 ng p24/ml) and X4-tropic (HXB2) virions (27 ng p24/ml).

(C) PS exposure at the surface of HeLa45 cells with varied expression and function of TMEM16F (see also Figure S3). Cell-surface PS after virus (JR-FL, 39 ng p24/ml) application and without it for HeLa45 cells, which along with CD4 and CCR5 and endogenous TMEM16F express: control shRNA (1), TMEM16F-silencing shRNA (2), TMEM16F-silencing shRNA together with shRNA-resistant form of the TMEM16F (3), WT TMEM16F (4), and constitutively active mutant TMEM16F (5).

(B and C) In each experiment, LactC2 fluorescence was normalized to that in the control experiment without virus (bar 1). Data are presented as means with 95% confidence intervals.

that support viral entry and infection. Since disrupting the PS externalization pathway suppressed HIV-1 infection, this pathway may present new targets for development of anti HIV-1 drugs.

RESULTS

Env-Coreceptor Interactions Trigger PS Externalization in the Target Cell

For most mammalian cells, the outer leaflet of the plasma membrane normally contains no detectable amounts of PS (Fadeel and Xue, 2009). As expected, the amounts of PS at the surface of Jurkat cells expressing CD4, CXCR4, and CCR5 (JkT-CCR5 cells) (Morcock et al., 2005) were very low (Figures 1A and 1B), as evidenced by a near-background staining with a sensitive PS probe, the fluorescently labeled C2 domain of lactadherin (LactC2) (Otzen et al., 2012). Application of GFP-labeled pseudoviruses carrying CXCR4 (X4)- or CCR5 (R5)-tropic HIV-1 Env induced a robust exposure of PS at the surfaces of some cells within 5–7 min after virus application (Figure S1). The extents and rates of PS exposure varied widely among individual cells. Note that in these experiments, we used high amounts of virus to reliably characterize the effects of the inhibitors of PS externalization.

The virus-induced PS externalization strictly depended on gp120-coreceptor engagement. CCR5 antagonist TAK-779 that blocks gp120-CCR5 interactions and HIV-1 fusion (Kondru et al., 2008) inhibited PS exposure induced by R5-tropic virions but not by X4-tropic virions (Figure 1B). Conversely, AMD-3100, a CXCR4 antagonist (Hendrix et al., 2000), inhibited PS exposure induced by X4-tropic virions and had no effect on PS exposure induced by R5-tropic virus. Experiments in which recombinant gp120 was applied in lieu of HIV-1 pseudovirus gave similar results (Figure S2), demonstrating that specific interactions of gp120 with coreceptors are sufficient to trigger PS externalization.

We then explored whether HIV-1 pseudovirus-induced PS externalization involves TMEM16F. CaCCinh-A01 (A01), an inhibitor of TMEM16 channels, suppressed PS exposure induced both by virions and by recombinant gp120, irrespective of coreceptor tropism (Figures 1A, 1B, and S2). Since A01 can influence other members of the CaCC protein family, the specific dependence of HIV-1-induced PS externalization on TMEM16F was confirmed by the experiments in which we varied the levels of expression and activity of this protein in HeLa45 cells (HeLa-derived cells expressing CD4 and CCR5) (Figures 1C and S3 and Table S1). Virus-induced PS exposure at the surface of HeLa45 cells transduced with the TMEM16F-silencing shRNA was lower than at the surface of the cells expressing control shRNA. The PS exposure was rescued in cells expressing TMEM16F-silencing shRNA together with the shRNA-resistant TMEM16F construct. In a complementary approach, we found that boosting the function of TMEM16F in HeLa45 cells by overexpression of wild-type (WT) TMEM16F, and especially by overexpression of the constitutively active TMEM16F mutant (Segawa et al., 2011), increased PS exposure.

In summary, specific interactions of the gp120 subunit of HIV-1 Env with coreceptors trigger TMEM16F-mediated PS externalization.

PS Dependence of Env-Mediated Cell-Cell Fusion

Having established that HIV-1 induces PS externalization, we asked whether this process influences Env-mediated membrane fusion. HeLa cells that express the R5-tropic HIV-1 ADA Env (Env

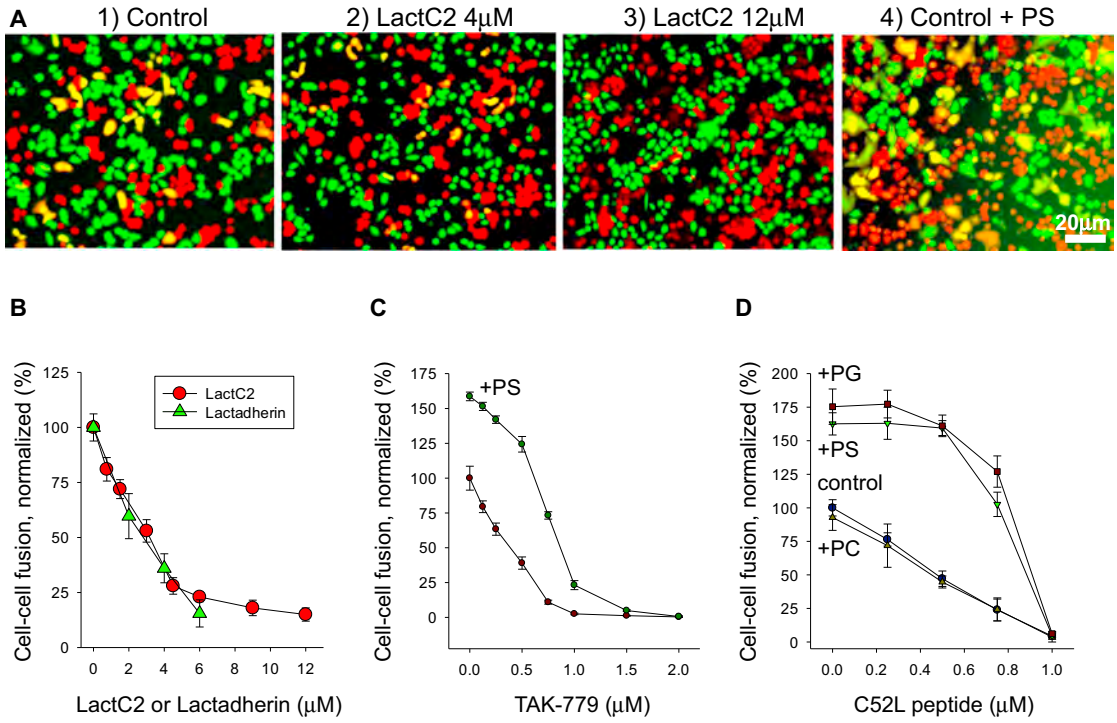

Figure 2. HIV-1 Env-Mediated Cell-Cell Fusion Depends on PS

(A) Blocking of accessible PS with LactC2 inhibits fusion, and adding exogenous PS promotes fusion. Fluorescence microscopy images of co-plated mCherry-labeled Env cells (red) and eGFP-labeled TZM-bl cells (green). The cells were treated with 4 or 12 μM LactC2, exogenous PS, or left untreated. Fused cells are seen as co-labeled (yellow) cells.

(B) PS-binding LactC2 and full-length lactadherin inhibit fusion.

(C and D) Exogenous PS (C and D) and PG (D), in contrast to PC (D), promote fusion and increase fusion-inhibiting concentrations of TAK-779 (C) and C52L (D).

(B–D) Fusion extents measured by fusion-per-contact assay were normalized to those observed for untreated cells. All results are means ± SEM ($n \geq 3$).

cells) (Pleskoff et al., 1997) were co-incubated with TZM-bl cells, which express high levels of CD4 and CCR5 (Harmon et al., 2010; Platt et al., 1998). Fusion between target cells stably expressing eGFP and Env cells expressing mCherry was detected as an appearance of cells positive for both cytoplasmic markers. If Env-mediated fusion depends on endogenous PS in the outer leaflet of the plasma membrane, we expect fusion to be inhibited by PS-binding proteins. Indeed, we found that LactC2 and full-length lactadherin inhibited Env-mediated fusion (Figures 2A and 2B).

The dependence of Env-mediated fusion on externalized PS suggests that exogenous PS can promote fusion. Indeed, addition of exogenous PS to the mixture of Env cells and TZM-bl cells promoted their fusion (Figures 2A, 2C, and 2D). The enhancing effect was especially substantial when fusion was partially suppressed with moderate concentrations of TAK-779 (for instance, 7-fold promotion in the presence of 0.75 μM TAK-779 versus 1.6-fold promotion in the absence of the reagent) (Figure 2C). Similarly, we found that PS application increased fusion more strongly in the presence of a partially inhibiting concentration of C52L peptide, an inhibitor of Env-mediated fusion that blocks gp41 restructuring into the post-fusion 6-helix bundle conformation (Deng et al., 2007) (Figure 2D). Importantly, high concentrations of TAK-779 and the C52L peptide abrogated Env-mediated fusion between the cells supplemented with PS, demonstrating that cell fusion after PS application retained complete dependence on gp120-coreceptor interactions and gp41 restructuring. Promotion of Env-mediated cell-cell fusion was also observed for cells expressing X4-tropic Env (Figure S4A). As expected, this fusion was inhibited by AMD-3100 and was insensitive to TAK-779.

A stronger PS promotion of fusion in the presence of moderate concentrations of coreceptor antagonist suggested that lowering of the surface density of coreceptors will enhance the PS promotion. Indeed, replacing TZM-bl cells, characterized by a very high expression of CCR5, with JC.10 cells, which have much lower levels of CCR5 expression (2×10^3 versus 10^5 CCR5/cell; Platt et al., 1998) strongly increased the extent of the fusion promotion by exogenous PS (~6-fold in Figure S4B versus ~1.6-fold in Figure 2C with no TAK-779).

Application of another anionic lipid, phosphatidylglycerol (PG), with a polar group markedly different from that of PS, also promoted cell fusion (Figure 2D). In contrast, zwitterionic lipid phosphatidylcholine (PC) had no effect, suggesting that Env-mediated fusion is promoted by the increased negative charge of the external leaflets rather than by a specific polar head group of a lipid.

To summarize, blocking accessible endogenous PS at the cell surface decreased, and application of exogenous PS increased the efficiency of Env-mediated cell fusion. The extent of fusion promotion by exogenous PS depended on the number of fusion-competent Envs. Lowering the number of Envs engaged with CD4 and coreceptor and the gp41 subunits

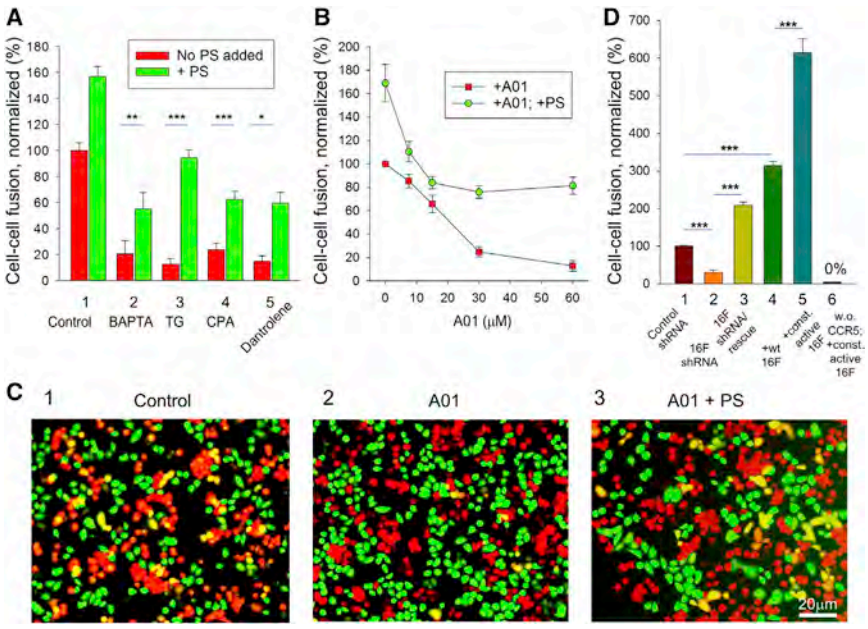

Figure 3. Interfering with Cell Signaling Pathways Involved in PS Exposure Inhibits Env-Mediated Cell-Cell Fusion

(A) Fusion inhibition by blocking the elevation of intracellular calcium with BAPTA-AM (10 μM), thapsigargin (TG, 2 μM), cyclopiazonic acid (CPA, 10 μM), and dantrolene (100 μM) was partially rescued by exogenous PS.

(B) Fusion inhibition by suppressing PS externalization with A01 was partially lifted by PS.

For (A) and (B), fusion between mCherry-labeled Env cells (red) and eGFP-labeled TZM-bl cells (green) was measured by the fusion-per-contact assay, and fusion extents were normalized to those in the experiments with the untreated cells.

(C) Fluorescence microscopy images of the contacting Env cells and TZM-bl cells illustrate inhibition of cell fusion (a decrease in the number of yellow cells) by 60 μM A01 (image 2 versus image 1) and partial recovery of the fusion for the A01-treated cells after PS application (image 3 versus 2).

(D) Fusion between Env cells and HeLa45 cells with modified expression of TMEM16F was assayed with the fusion-per-target-cell assay. Fusion extents for the target cells expressing TMEM16F-silencing shRNA (2), TMEM16F-silencing shRNA together with shRNA-resistant TMEM16F (3), WT TMEM16F (4), and constitutively active mutant TMEM16F (5) were normalized to those in the experiments with the HeLa45 cells expressing control shRNA (bar 1). (6) HeLa4 cells expressing CD4 and constitutively active mutant TMEM16F, but not expressing CCR5. All results are means ± SEM ($n \geq 3$). Levels of significance relative to controls (bar 1) are shown: *$p < 0.05$, **$p < 0.01$, and ***$p < 0.001$.

able to undergo fusogenic restructuring with moderate concentrations of TAK-779 or C52L, or using the target cells with lower levels of coreceptor expression, resulted in an especially notable PS promotion.

Env-Mediated Cell-Cell Fusion Depends on Ca^{2+} Signaling and TMEM16F Activity in the Target Cells

HIV-1 Env-coreceptor interactions trigger signaling pathways that involve a transient rise in intracellular Ca^{2+} (Harmon et al., 2010; Harmon and Ratner, 2008; Melar et al., 2007). Can the established role of some of these signaling pathways in Env-mediated fusion reflect the PS dependence of fusion? We found Env-mediated cell fusion to be inhibited by BAPTA AM, a membrane permeable chelator of intracellular Ca^{2+} (Figure 3A). In agreement with Harmon and Ratner (2008), thapsigargin and cyclopiazonic acid that block a rise in intracellular Ca^{2+} by depleting internal Ca^{2+} stores inhibited fusion. In addition, dantrolene, an inhibitor of intracellular Ca^{2+} release (Zhao et al., 2001), also suppressed fusion. Addition of exogenous PS rescued fusion suppressed by all these inhibitors of Ca^{2+} signaling, suggesting that these signaling pathways, at least partially, influence Env-mediated fusion by delivering PS to the cell surface.

The importance of virus-triggered Ca^{2+}-dependent PS exposure was further confirmed by experiments in which we targeted the activity and expression of TMEM16F. A01, an inhibitor of TMEM16F-mediated PS externalization, suppressed Env-mediated cell fusion in a dose-dependent manner (Figures 3B and 3C). PS application partially restored fusion efficiency. In a complementary approach, we compared the dependence of fusion on TMEM16F expression in the target cells. TMEM16F shRNA expression in HeLa45 cells inhibited fusion (Figure 3D). Fusion was rescued for the HeLa45 expressing TMEM16F-silencing shRNA together with shRNA-resistant TMEM16F. HeLa45 cells with boosted TMEM16F expression demonstrated higher fusion efficiency than the parental HeLa45 cells expressing only endogenous TMEM16F. Fusion was even stronger for HeLa45 cells expressing the constitutively active TMEM16F mutant. No fusion was observed for the HeLa4 target cells expressing CD4 and constitutively active TMEM16F but no CCR5. While the levels of expression of CD4 and CCR5 on HeLa45 cells with modified expression of TMEM16F were not identical (Figure S4C), similar variations in the levels of CD4 and CCR5 between different clones of HeLa45 did not appreciably alter the fusion efficiency (Figures S4C and S4D). Thus, the differences in fusion efficiency for target cells with modified TMEM16F expression indicated that cell-cell fusion depends on TMEM16F activity rather than on modulation of receptor and coreceptor levels.

To summarize, our data suggest that Env-mediated cell fusion involves Ca^{2+}-signaling-dependent TMEM16F-mediated PS externalization.

The PS-Dependent Stage Precedes gp41 Refolding and Hemifusion

Membrane fusion proceeds through several distinct stages. Merger of the outer leaflets of membranes at the early fusion stage, referred to as hemifusion (Chernomordik and Kozlov, 2005), allows lipid mixing. Subsequent opening of a fusion pore allows mixing of the volumes enclosed by the two membranes. We found that A01 inhibited not only content mixing, but also lipid mixing between the membranes of two cells (Figures 4A and 4B), suggesting that the PS-dependent fusion stage precedes hemifusion.

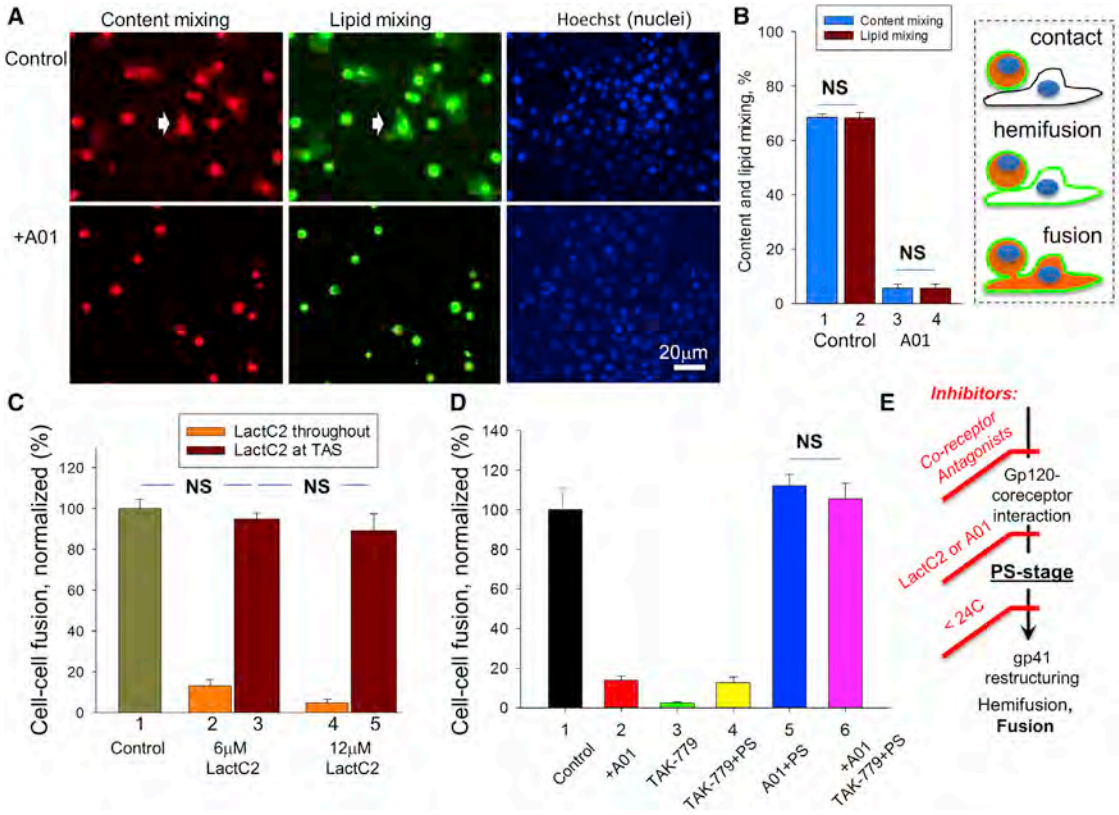

Figure 4. PS-Dependent Fusion Stage Follows gp120-Coreceptor Interactions and Precedes Hemifusion

(A and B) An inhibitor of PS externalization, A01 (60 μM), suppresses both content and lipid mixing and thus blocks Env-mediated cell fusion upstream of hemifusion. (A) Fluorescence microscopy images of a few Env cells labeled with both RFP (red, content probe) and Vybrant DiI (green, membrane probe) bound to the adherent TZM-bl cells labeled with Hoechst 33342 (blue). Arrows mark a cell after completed fusion event (an adherent cell labeled with both membrane and content probes). As illustrated in the cartoon on the right, fusion arrest at a stage between hemifusion and fusion completion would produce adherent cells that acquired green membrane probe but not red content probe. (B) Content and lipid mixing extents quantified as described in STAR Methods were normalized to the number of Env cells.

(C) LactC2 inhibits fusion, if present throughout cell interactions and fusion (bars 2 and 4). It does not inhibit fusion if applied to the cells accumulated for 3 hr at the temperature-arrested stage (TAS) at the time of raising the temperature to 37°C (bars 3 and 5).

(D) Downstream of the PS-dependent stage, fusion progression does not require additional gp120-coreceptor engagements. The fusion block for 60 μM A01-treated cells was (still in the presence of A01) lifted by application of exogenous PS with (6) or without (5) 1 μM TAK-779. Controls in which the cells were untreated (1), treated with A01 (2), treated with TAK-779 (3), and treated with TAK-779 and PS (4).

For (C) and (D), fusion extents measured by fusion-per-contact assay were normalized to those observed for untreated cells. All results are means ± SEM ($n \geq 3$). NS, no significant difference.

(E) Our data place the PS-dependent fusion stage blocked by LactC2 and A01 downstream of gp120 interactions with coreceptors blocked by coreceptor antagonists and upstream of the temperature-dependent transition from assembled gp120-CD4-coreceptor to gp41 restructuring blocked at the TAS.

To examine which of the pre-hemifusion stages of Env-mediated fusion depends on PS, we used approaches developed earlier in our laboratories (Chernomordik and Kozlov, 2005; Melikyan, 2008). In particular, we focused on intermediates accumulated after a 3 hr co-incubation of Env cells with TZM-bl cells at 22°C (temperature-arrested stage; TAS). We also captured fusion in the presence of lysophosphatidylcholine (LPC) at a stage upstream of hemifusion, referred to as an LPC-arrested stage (LAS). In the TAS intermediates, Env-CD4-coreceptor complexes are already formed, but there is as yet no direct interaction between gp41 and the target membrane (Melikyan, 2008). In contrast, LAS is created at 37°C, which likely allows gp41-membrane engagement, but blocks the merger of the contacting leaflets of fusing membranes (Melikyan, 2008). As shown above, LactC2 application at the time Env cells were brought into contact with the target cells inhibited cell-cell fusion. However, LactC2 added at the time of raising the temperature to 37°C after establishment of TAS did not inhibit cell fusion (Figure 4C), nor did it affect fusion when added after cells captured at LAS were allowed to fuse by removal of LPC (Figure S4E). Exogenous PS applied to the cells arrested at LAS also had no effect on fusion. This finding indicates that the PS-dependent stage precedes an actual membrane merger event.

To further characterize the PS-dependent fusion stage, we treated an Env cell-TZM-bl cell co-culture with A01 to block externalization of endogenous PS, resulting in accumulation of fusion intermediates upstream of the PS-dependent stage (Figure 4D). As shown above, subsequent application of exogenous PS, still in the presence of A01, rescued fusion. Importantly, fusion was rescued even when PS was applied together with

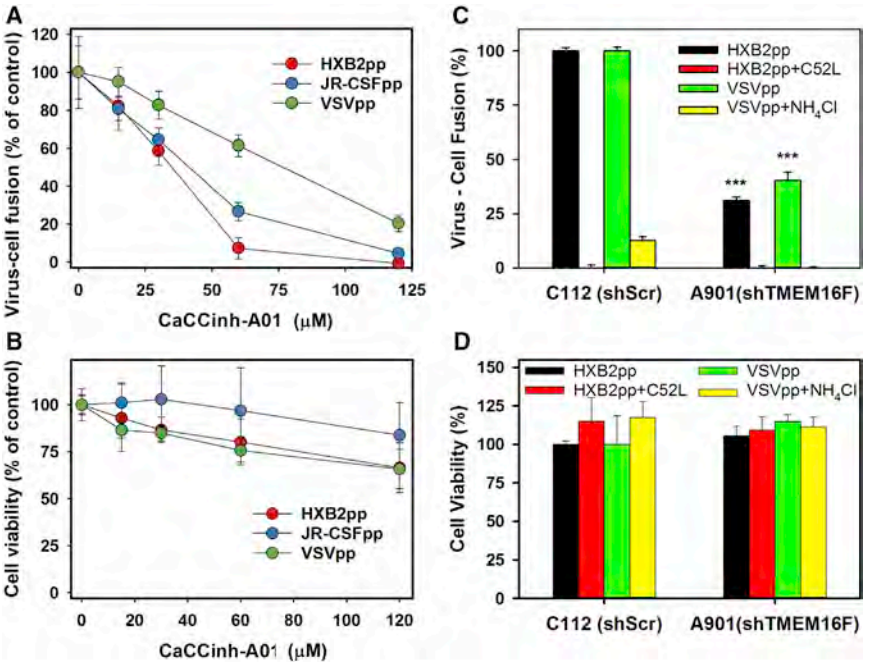

Figure 5. The Dependence of HIV-1 Virus-Cell Fusion on TMEM16F Activity

(A and B) Effects of A01 on virus-cell fusion (A) and cell viability (B) for the pseudotyped HIV-1 particles HXB2pp or JR-CSFpp (red and blue circles, respectively) or for VSV G-pseudotyped particles (VSVpp, green) measured as BlaM activity. Pseudoviruses at MOI of ~1 (5 ng p24/ml for HXB2 and VSV-G, and 6 ng p24/ml for JR-CSF) were bound to adherent TZM-bl cells in the cold, and fusion was allowed to proceed for 90 min at 37°C.

(C and D) The knockdown of TMEM16F using shRNAs in JkT-CCR5 cells significantly inhibits HIV-1- and VSV-cell fusion (C) but does not lower cell viability (D).

For (C), the pseudoviruses were added to cells at MOI of ~3 (15 ng p24/ml). C52L (1 μM) and acidification inhibitor NH_4Cl (70 mM) were used as controls for HIV-1 and VSV fusion. Data points are means ± SEM of two independent triplicate experiments. ***$p < 0.001$.

TAK-779, an inhibitor of gp120-CCR5 binding, and thus, PS-mediated promotion cannot be explained by the engagement of additional coreceptor molecules by Env.

We conclude that the PS-dependent stage of Env-mediated fusion follows the formation of pre-fusion Env-CD4-coreceptor complexes and precedes the gp41 restructuring, which brings about hemifusion and fusion (Figure 4E).

Virus-Cell Fusion and Viral Entry Depend on TMEM16F-Mediated PS Externalization

Not all features of the virus fusion stage of entry can be faithfully reproduced in cell-cell fusion model (Connolly and Lamb, 2006). We verified that the dependences of Env-mediated fusion on PS and TMEM16F were also observed for virus-cell fusion. We therefore examined the effects of A01 and TMEM16F suppression on HIV-1 pseudovirus fusion with cells by measuring the cytosolic activity of the viral core-associated β-lactamase (Miyauchi et al., 2009). As in the case of Env-mediated cell-cell fusion, A01 inhibited fusion of viruses bearing X4-tropic HXB2 Env or non-macrophage R5-using JR-CSF Env, which, similarly to most HIV-1 transmitted/founder viruses, requires high CD4 levels on target cells (Ping et al., 2013; Shaw and Hunter, 2012) (Figure 5A). Virus fusion to Jurkat-derived cells, in which TMEM16F expression was silenced by shRNA (A901 cells), was less efficient than virus fusion to the control C112 cells (Figure 5C). Suppressing the expression or activity of TMEM16F also inhibited fusion of a pseudovirus bearing VSV G (Figures 5A and 5C). Neither moderate concentrations of A01 nor knocking down TMEM16F significantly lowered the cell viability (Figures 5B and 5D). We also verified that A01 had no virucidal activity, i.e., did not inactivate HIV-1 pseudoviruses on contact (Figure S5A). These findings suggest that virus-cell fusion mediated by HIV-1 Env and, to a somewhat lesser extent, by VSV G protein depends on activity of TMEM16F and on PS. We tested PS dependence of VSV G-mediated low pH triggered cell-cell fusion and found this fusion to be inhibited by blocking cell-surface PS with LactC2 and promoted by adding PS (Figure S5B). These findings indicate that PS influences VSV fusion rather than pre-fusion stages of VSV entry.

We then explored the importance of PS externalization and TMEM16F in HIV-1 entry. As in the case of Env-mediated cell-cell fusion, blocking accessible PS on the cell surface with LactC2 inhibited entry of HIV-1 pseudoviruses, assayed as single-round infection of JkT-CCR5 cells with HIV-1 pseudoviruses (Figures 6A and 6B). Pre-treating the JkT-CCR5 cells with A01 also inhibited the entry of HIV-1 pseudoviruses carrying Env of X4-tropic (HXB2) and R5-tropic (JR-FI and BaL) HIV-1 strains (Figure 6C). LactC2 and A01 also inhibited the entry for pseudovirus bearing the JR-CSF Env. Since this virus did not infect JkT-CCR5 cells, these experiments have been carried out with TZM-bl cells (Figures 6D and 6E) and with U87.CD4.CCR5 cells (Figures S5C and S5D).

Infectivity was reduced in cells expressing TMEM16F shRNA and was rescued in cells expressing exogenous TMEM16F refractory to aforementioned shRNA (Figure 6F). Increased PS exposure caused by overexpression of WT TMEM16F promoted HIV-1 pseudovirus infection. Promotion was even stronger for the target cells expressing a constitutively active mutant of TMEM16F. These findings confirmed the importance of TMEM16F in viral entry.

Changes in the extents of virus infection can reflect changes in the efficiency of virus-cell binding (Platt et al., 2010). We therefore tested whether elevated PS externalization correlated with a more efficient cell surface attachment of Gag-Ruby-labeled virions (Figure S6A). Virus attachment to cells with inhibited TMEM16F function (HeLa45 cells treated with A01 or expressing TMEM16F shRNA) was not affected. We also did not detect promotion of virus attachment to cells overexpressing WT TMEM16F or its constitutively active mutant. These findings suggested that the dependence of viral entry on PS exposure cannot be explained by changes in virus attachment to the cell surface.

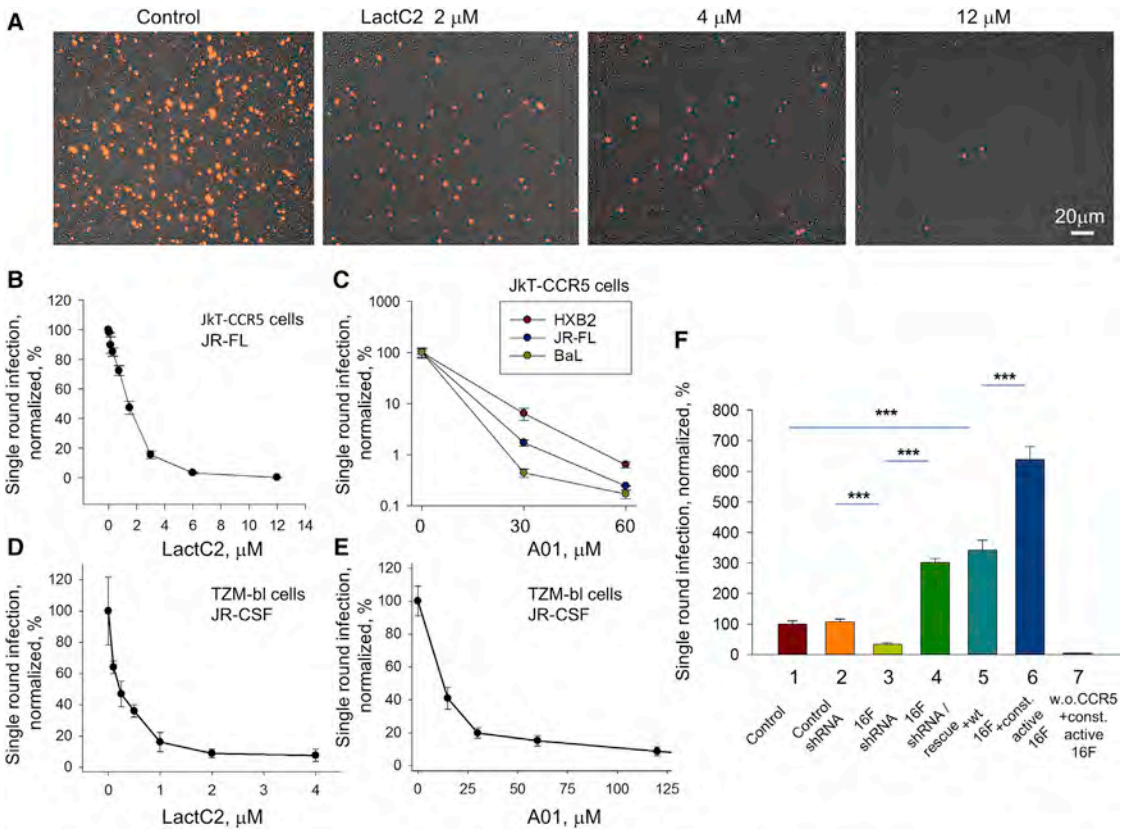

Figure 6. Single-Round Infection with HIV-1 Pseudovirus Depends on PS Externalization in the Target Cells

(A and B) Blocking accessible PS with LactC2 inhibits infection of JkT-CCR5 cells by RFP-encoding HIV-1 pseudoviruses (JR-FL) at MOI of 0.5 (0.4 ng p24/ml). The fluorescence microscopy images of infected cells (red) (A) were taken and analyzed (B) 72 hr post-infection.

(C) The effects of A01 pretreatment of Jurkat cells on the infection at MOI of 0.5 by RFP-encoding pseudoviruses carrying Env of three HIV-1 strains: X4-tropic HXB2 (2.7 ng p24/ml), R5-tropic JR-FL (0.4 ng p24/ml), and BaL.01 (0.44 ng p24/ml).

(D and E) Inhibition of infection of TZM-bl cells with JR-CSF HIV-1 pseudovirus at MOI of 0.5 (6 ng p24/ml) with LactC2 (D) and with A01 pretreatment of the cells (E).

(F) The efficiency of RFP-encoding JR-FL virus infection (MOI of 0.5; 0.42 ng p24/ml) of the cells with modified expression of TMEM16F. Percentages of infected (RFP-labeled) cells were measured for the target HeLa45 cells expressing control siRNA (2), TMEM16F-silencing shRNA (3), TMEM16F-silencing shRNA together with shRNA-resistant TMEM16F (4), WT TMEM16F (5), and constitutively active mutant TMEM16F (6). The data were normalized to those in the control experiment with HeLa45 cells with unmodified expression of TMEM16F (1).

(B–F) The average numbers of infected cells per field of view at 72 hr post-infection were normalized to those in the control experiment with neither LactC2 (B and D) nor A01 (C and E) applied or to the control experiment with HeLa45 cells with unmodified expression of TMEM16F (1; F). All results are means ± SEM (n = 4). (F) Level of significance relative to controls (bar 1) is shown: ***$p < 0.001$.

In conclusion, HIV-1 fusion and single-round infection depend on TMEM16F and cell-surface PS.

HIV-1 Replication Depends on TMEM16F Activity

We next investigated whether TMEM16F is involved in the replicative infection of a prototypic X4 HIV-1 strain, LAI.0.4. We compared $HIV_{LAI.04}$ infection of JkT-CCR5-derived cells, in which TMEM16F expression was silenced by shRNA (A901 cells), with infection of control C112 cells (Figures 7A–7F). The cells were inoculated with various amounts of virus (from 0.05 to 5 ng of p24 per 10^5 cells in 200 μl). At day 3, the number of infected cells (p24+) depended on the size of the inoculum for both cell lines. For high amount of viral inoculum (5ng of p24), the fraction of infected cells was almost 10-fold lower in A901 cells than in C112 cells (Figure 7A). For C112 cells at day 7, the percentage of infected cells reached a plateau (around 65%) irrespective of the viral inoculum, whereas in A901 cells the number of infected cells depended on the viral inoculum amount (Figures 7D–7F). For high amount of viral inoculum (5 ng of p24), the infection level in A901 cells remained 2.5-fold lower than that in C112 cells (Figures 7D and 7G). Lowering the amount of the inoculum to 0.05 ng of p24 only marginally affected the level of infection at day 7 in C112 cells (Figures 7D and 7F), while the infection in A901 cells was markedly decreased and the difference in the infection levels between A901 and C112 cells rose to almost 6-fold (Figure 7F). These data indicate that HIV-1 infection depended on TMEM16F expression and that this dependence was stronger at early time points and at lower virus concentrations in the inoculum.

Since critical events of HIV-1 pathogenesis *in vivo* occur in lymphoid tissues, we investigated whether suppression of TMEM16F activity affects HIV-1 infection of human lymphoid

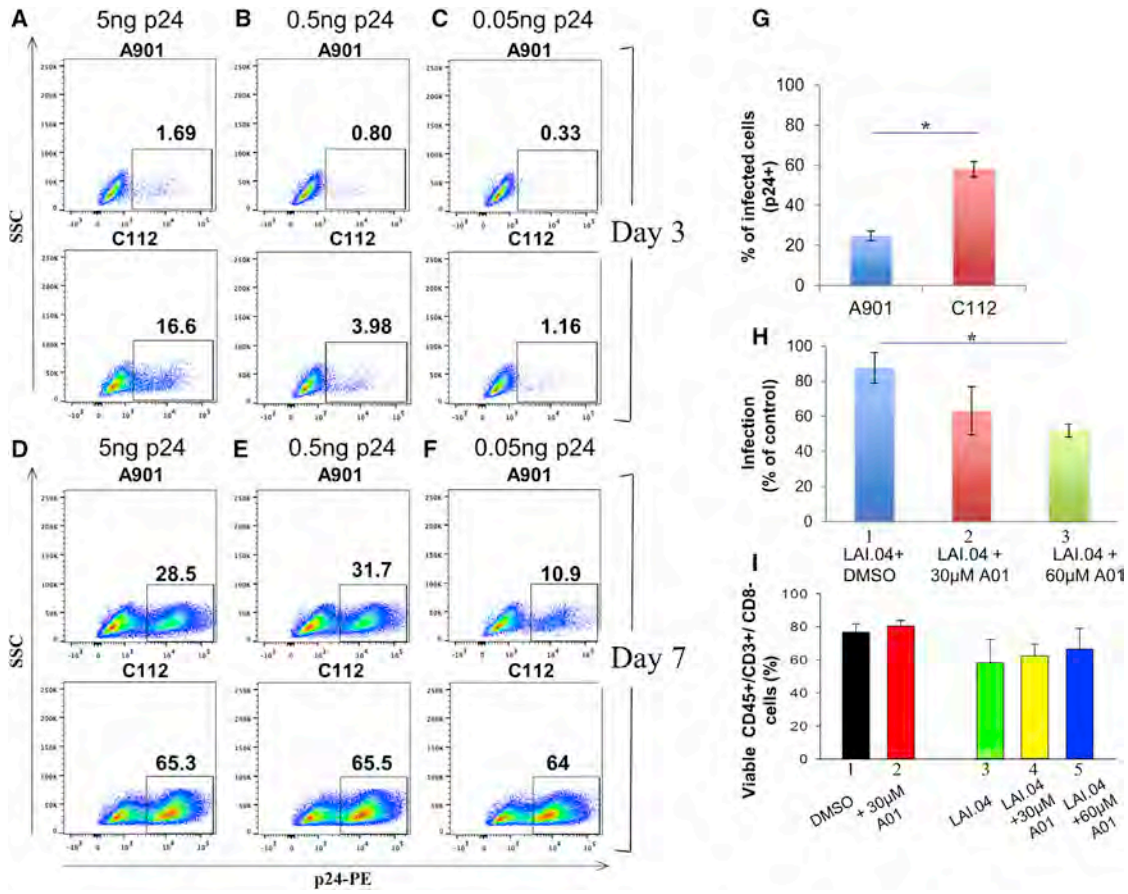

Figure 7. Productive Infection with HIV-1 Depends on TMEM16F Activity

(A–F) Jurkat cells expressing either TMEM16F shRNA (A901 cells A–F upper panel) or control shRNA (C112 cells; A–F lower panel) were inoculated with $HIV_{LAI.04}$ at 5 ng (A and D), 0.5 ng (B and E), or 0.05 ng of p24 (C and F) per 10^5 cells in 200 μl. Infection was evaluated from intracellular staining for p24 at days 3 (A–C) and 7 (D–F) post-infection.

(G) Comparison between the percentages of infected A901cells and C112 cells at day 7 post-infection. Means ± SEM of two experiments.

(H) Suppression of TMEM16F activity inhibits $HIV_{LAI.04}$ infection of human lymphoid tissue *ex vivo*. Human tonsillar tissue blocks were inoculated with $HIV_{LAI.04}$ with 5 μl of $HIV_{LAI.04}$ viral stock (50 ng of p24/ml) per tissue block; DMSO or A01 was applied at 30 or 60 μM. Tissue cultures were monitored for 12 days, and medium was collected and replaced every 3 days, with replenishment of fresh A01. Virus production was evaluated from measurement of p24 accumulated in the culture medium. Infection was normalized to that in untreated tissue.

(I) The effects of A01 on the viability of the target cells were characterized by comparing the percentages of viable CD45+/CD3+/CD8− cells without virus (bars 1 and 2) and after infection (bars 3–5).

(G–I) Means ± SEM (n = 2). Statistical significant difference relative to controls (bars 1) *$p < 0.05$.

tissue *ex vivo*. In this system, lymphoid tissue retains its 3D organization and supports HIV-1 infection without exogenous activation or stimulation. This model also recapitulates several important aspects of tissue infection *in vivo* (Grivel and Margolis, 2009). Here, we inoculated human tonsillar tissue blocks with $HIV_{Lai.04}$ with A01 or without it. Tissue cultures were monitored for 12 days, and medium was collected and replaced every 3 days, with replenishment of fresh A01. Virus production was evaluated by measuring p24 accumulated in the culture medium of A01-treated and non-treated cells. While in this model the effects of A01 can be limited by its stability and inaccessibility of some target cells in the tissue, $HIV_{Lai.04}$ replication in the A01-treated tonsillar tissue was significantly lower than in the tissues treated with DMSO (vehicle control) (Figure 7H). This inhibition cannot be explained by any decrease in the numbers of cells targeted by HIV-1. We found similar percentages of viable CD45+/CD3+/CD8− cells in the tissue blocks cultured with or without A01 (Figure 7I).

In summary, our findings on live HIV-1 infection in JkT-CCR5-derived cells and in *ex vivo* tissues are consistent with the suggested role of TMEM16F in HIV-1 entry.

DISCUSSION

To prevent premature release of the energy stored in a metastable native conformation of HIV-1 gp41 (Weissenhorn et al., 1997) and to identify appropriate target cells, HIV-1 utilizes a multistep activation of its fusion machinery (Wilen et al., 2012). This activation requires the target membrane to present several distinct cofactors. Here, we show that, in addition to CD4 and chemokine receptors, restructuring of gp41 and membrane fusion depend on PS exposure at the surfaces of target cells.

The HIV-1 gp120 interactions with coreceptors trigger intracellular Ca^{2+}-dependent TMEM16F-mediated redistribution of PS from the inner to the outer leaflet of the plasma membrane. It is well known that HIV targets predominantly activated target cells (Lackner et al., 2012). Cell activation is a complex and poorly defined process that includes an increase in cytokine release and upregulation of certain plasma membrane molecules such as CD25, CD69, and HLA-DR. The exact mechanisms by which various aspects of cell activation facilitate HIV-1 infection remain to be understood. Our work suggests that one of these mechanisms is based on the dependence of HIV-1 entry on PS signaling, a known hallmark of several pathways of activation of immune cells (Chaurio et al., 2009; Elliott et al., 2005; Fischer et al., 2006). The dependence of the fusion stage of HIV-1 infection on PS may focus the viral infection on CD4- and coreceptor-expressing cells of a certain activation status conducive to PS signaling and infection.

The PS-Dependent Stage in the HIV-1 Fusion Pathway

Several earlier studies have suggested that PS may influence HIV-1 infection. Liposomes containing PS and other anionic lipids, depending on experimental conditions, inhibit (Callahan et al., 2003; Malavia et al., 2011) or promote HIV-1 fusion and infection (Larsen et al., 1993; Lenz et al., 2005). Moreover, HIV-1 particles budded from infected cells undergoing apoptosis display PS on viral envelope, and this viral PS, apparently by engaging specific receptors on macrophages, promotes macrophage infection (Callahan et al., 2003). In an essential distinction from these studies, our work reports and explores the dependence of the HIV-1 fusion and infection on PS at the surfaces of non-apoptotic target cells and the signaling pathways that deliver PS to the surface of these cells. This dependence is conserved between X4-tropic viruses and R5 viruses, including physiologically relevant high CD4-requiring, non-macrophage-tropic R5 virus JR-CSF (Ping et al., 2013). Fusogenic restructuring of the gp41 subunits of the Env trimer from their initial conformation to the post-fusion 6-helix bundle conformation requires weakening of gp41–gp120 interactions triggered by assembly of the pre-fusion gp120-CD4-coreceptor complex. Our data suggest that PS in the target membrane acts downstream of gp120-coreceptor interactions but upstream of gp41 engagement of the target membrane.

PS exposure and associated loss of the phospholipid asymmetry are likely accompanied by changes in the physical properties of membranes. These changes could facilitate receptor engagement with gp120 by supporting specific conformations of the CD4 and coreceptors. However, we consider this interpretation unlikely, since fusion intermediates accumulated upstream of the PS-dependent stage, and then, supplemented with exogenous PS, proceeded to fusion in the presence of TAK-779 and thus without additional gp120-coreceptor engagements.

A similar promotion of Env-mediated fusion by PS and PG suggested the importance of electrostatic interactions rather than specific interactions with the polar head group of PS. We propose that PS at the surface of the target cell lowers the minimal number of coreceptor molecules that need to be engaged by each Env trimer to initiate gp41 refolding. The negatively charged PS on the target membrane can draw out the positively charged regions of a coreceptor-free gp120 monomer that are exposed after gp120-CD4 binding (Kwong et al., 2000). These electrostatic interactions may stabilize intermediate conformations of gp120 and facilitate gp41 release from the gp120 grip. An especially strong fusion promotion by exogenous PS for the target cells with relatively low density of accessible CCR5 (Figures 2C and S4B) may reflect a stronger dependence of their fusion on gp120 trimer-coreceptor complexes with fewer than three engaged coreceptors. However, fusogenic restructuring of Env depends on cell-surface PS and thus can be inhibited by A01 and LactC2 and promoted by exogenous PS, even for target cells with exceptionally high levels of CCR5 expression such as TZM-bl cells (Platt et al., 2009). A very strong dependence of HIV-1 fusion on surface PS and, by extension, on the signaling triggered by Env-coreceptor interactions observed for the JC10 cells with low coreceptor densities ($\sim 2 \times 10^3$ CCR5/cell; Platt et al., 1998), approaching those characteristic for resting peripheral blood lymphocytes ($\sim$600 CCR5/cell; Blumenthal et al., 2012), is consistent with the hypothesis that signal transduction is essential in physiologically relevant conditions (reviewed in Wilen et al., 2012).

Virus-Induced PS Externalization and Viral Infection

Our work shows that HIV-1 does not passively rely on the presence of PS on the cell surface but actively entices cells to externalize PS through interactions between gp120 and coreceptors. These interactions activate phospholipid scramblase TMEM16F and PS externalization. Our finding that application of exogenous PS rescues Env-mediated fusion inhibited by A01 suggests that fusion depends on PS externalization activity rather than on channel activity of any TMEM16 proteins. The Ca^{2+} dependence of PS externalization suggests a new interpretation for reported dependences of HIV-1 fusion on Ca^{2+} signaling (Harmon and Ratner, 2008). However, incomplete restoration of fusion suppressed by the inhibitors of Ca^{2+} signaling by exogenous PS may indicate that, along with PS externalization, Ca^{2+} signaling influences HIV-1 fusion and entry in some other ways, for instance by activating Rac-1 GTPase (Harmon and Ratner, 2008).

Ca^{2+} signaling responses depend on the differentiation status of human T cells and drastically differ among individual cells, with some cells showing no Ca^{2+} elevation at all (Arrol et al., 2008; Robert et al., 2013). The extents of PS exposure also vary both between the individual JkT-CCR5 cells in the culture (Figure S1) and between freshly isolated T lymphocytes, where activated/memory CD4+ T cells present the highest levels of cell-surface PS (Elliott et al., 2005). We propose that the differences between PS externalization in distinct T cell subsets may contribute to the differences in the efficiencies of HIV-1 fusion and infection such as a lowered efficiency of fusion for naive versus memory resting $CD4^+$ T cells (Dai et al., 2009). Cells that demonstrate stronger Ca^{2+} signaling and PS externalization in response to HIV-1 binding may better support virus replication. Indeed, cells with a lower level of CD45 expression, a negative regulator of Ca^{2+} signaling, have been reported to show both stronger PS externalization (Elliott et al., 2005) and higher levels of HIV-1 replication (Baur et al., 1994).

PS dependence that we uncovered here for HIV-1 entry can be shared by some other viruses. Early stages of cell infection by several flaviviruses depend on a sustained rise in intracellular Ca^{2+} (Scherbik and Brinton, 2010). The binding of the

alpha-herpesvirus envelope glycoprotein H to viral receptor induces Ca^{2+} signaling and PS exposure on the plasma membrane (Azab et al., 2015). Suppressing expression or activity of the TMEM16F scramblase diminishes VSV-cell fusion (Figure 5). This finding is consistent with an earlier study suggesting VSV G-PS interactions at the early stages of VSV G-mediated fusion (Carneiro et al., 2002), our finding that VSV G-mediated cell-cell fusion depends on cell surface PS (Figure S5B), and an earlier report that PS and/or other anionic lipids are required for single VSV particle fusion (Matos et al., 2013). The dependence of VSV fusion on the activity of TMEM16F scramblase may involve signaling pathways triggered by virus binding to its LDL-R receptor (Finkelshtein et al., 2013). Finally, the presence of PS in the target membrane promotes fusion for many viruses (Coil and Miller, 2005a, 2005b; Zaitseva et al., 2010). Both the specific mechanisms and the implications of the emerging coupling mechanism between intracellular signaling pathways and entry of different viruses remain to be clarified.

In summary, we demonstrated that the fusion stage of HIV-1 infection depends on a two-directional signaling pathway in which outside-in steps initiated by the virus at the plasma membrane are followed by inside-out steps, which deliver PS to the cell surface to promote the fusogenic restructuring of Env. Our findings suggest that the ability of the cells to mount PS signaling is an important aspect of immune cell activation and one of the controlling mechanisms for both productive and aborted infection of the cells.

STAR★METHODS

Detailed methods are provided in the online version of this paper and include the following:

- KEY RESOURCES TABLE
- CONTACT FOR REAGENT AND RESOURCE SHARING
- EXPERIMENTAL MODEL AND SUBJECT DETAILS
  - Cells
  - Pseudoviruses
  - Viruses
- METHOD DETAILS
  - Reagents
  - Plasmid Constructs
  - Clover-LactC2 Purification
  - Virus Binding
  - PS Externalization Assay
  - Cell-Cell Fusion
  - Hemifusion
  - Virus–Cell Fusion
  - Single-Round Infection
  - Infection with Live Virus
  - VSV G mediated Cell-Cell Fusion
  - Adding Exogenous Lipids
  - Temperature-Arrested Stage
  - Application of Inhibitors
- QUANTIFICATION AND STATISTICAL ANALYSIS

SUPPLEMENTAL INFORMATION

Supplemental Information includes seven figures and one table and can be found with this article online at http://dx.doi.org/10.1016/j.chom.2017.06.012.

AUTHOR CONTRIBUTIONS

Conceived and designed the experiments: E. Zaitseva, E. Zaitsev, A.A., M.M., K.M., L.B.M., G.B.M., and L.V.C. Performed the experiments: E. Zaitseva, E. Zaitsev, A.A., M.M., and R.V. Analyzed the data: E. Zaitseva, E. Zaitsev, K.M., A.A., M.M., G.B.M., L.B.M., and L.V.C. Wrote the paper: L.V.C., E. Zaitseva, E. Zaitsev, K.M., A.A., G.B.M., and L.B.M.

ACKNOWLEDGMENTS

We thank Dr. Jean-Charles Grivel for helpful discussions. The authors thank the NIH AIDS Reagent Program for cell lines and reagents, and are indebted to Drs. David Kabat, Gary E. Gilbert, Yuri Lazebnik, and Michel C. Nussenzweig for generous gifts of cells and constructs and to Drs. Dan Sacket and John Lloyd for their kind help with characterizing the purity of A01. The research in the L.V.C. laboratory was supported by the Intramural Research Program of the Eunice Kennedy Shriver National Institute of Child Health and Human Development, National Institutes of Health, by The Intramural AIDS Targeted Antiviral Program (2012-2014), and by the NICHD FY16 NICHD Intramural DIR/DIPHR HIV/AIDS Research Award, 2016. The research in the L.B.M. laboratory was supported by the Intramural Research Program of the Eunice Kennedy Shriver National Institute of Child Health and Human Development, National Institutes of Health. This work was also supported by NIH R01 GM054787 grant to G.B.M.

Received: October 7, 2016
Revised: March 13, 2017
Accepted: June 22, 2017
Published: July 12, 2017

SUPPORTING CITATIONS

The following references appear in the Supplemental Information: Binley et al. (2003); Gallay et al. (1996); Pietzsch et al. (2012); Platt et al. (2005); Shao et al. (2008).

REFERENCES

Arrol, H.P., Church, L.D., Bacon, P.A., and Young, S.P. (2008). Intracellular calcium signalling patterns reflect the differentiation status of human T cells. Clin. Exp. Immunol. *153*, 86–95.

Azab, W., Gramatica, A., Herrmann, A., and Osterrieder, N. (2015). Binding of alphaherpesvirus glycoprotein H to surface α4β1-integrins activates calcium-signaling pathways and induces phosphatidylserine exposure on the plasma membrane. MBio *6*, e01552–15.

Baur, A., Garber, S., and Peterlin, B.M. (1994). Effects of CD45 on NF-kappa B. Implications for replication of HIV-1. J. Immunol. *152*, 976–983.

Biancotto, A., Brichacek, B., Chen, S.S., Fitzgerald, W., Lisco, A., Vanpouille, C., Margolis, L., and Grivel, J.C. (2009). A highly sensitive and dynamic immunofluorescent cytometric bead assay for the detection of HIV-1 p24. J. Virol. Methods *157*, 98–101.

Binley, J.M., Cayanan, C.S., Wiley, C., Schülke, N., Olson, W.C., and Burton, D.R. (2003). Redox-triggered infection by disulfide-shackled human immunodeficiency virus type 1 pseudovirions. J. Virol. *77*, 5678–5684.

Blumenthal, R., Durell, S., and Viard, M. (2012). HIV entry and envelope glycoprotein-mediated fusion. J. Biol. Chem. *287*, 40841–40849.

Callahan, M.K., Popernack, P.M., Tsutsui, S., Truong, L., Schlegel, R.A., and Henderson, A.J. (2003). Phosphatidylserine on HIV envelope is a cofactor for infection of monocytic cells. J. Immunol. *170*, 4840–4845.

Carneiro, F.A., Bianconi, M.L., Weissmüller, G., Stauffer, F., and Da Poian, A.T. (2002). Membrane recognition by vesicular stomatitis virus involves enthalpy-driven protein-lipid interactions. J. Virol. *76*, 3756–3764.

Chaurio, R.A., Janko, C., Muñoz, L.E., Frey, B., Herrmann, M., and Gaipl, U.S. (2009). Phospholipids: key players in apoptosis and immune regulation. Molecules *14*, 4892–4914.

Chernomordik, L.V., and Kozlov, M.M. (2005). Membrane hemifusion: crossing a chasm in two leaps. Cell *123*, 375–382.

Coil, D.A., and Miller, A.D. (2005a). Enhancement of enveloped virus entry by phosphatidylserine. J. Virol. *79*, 11496–11500.

Coil, D.A., and Miller, A.D. (2005b). Phosphatidylserine treatment relieves the block to retrovirus infection of cells expressing glycosylated virus receptors. Retrovirology *2*, 49.

Connolly, S.A., and Lamb, R.A. (2006). Paramyxovirus fusion: real-time measurement of parainfluenza virus 5 virus-cell fusion. Virology *355*, 203–212.

Dai, J., Agosto, L.M., Baytop, C., Yu, J.J., Pace, M.J., Liszewski, M.K., and O'Doherty, U. (2009). Human immunodeficiency virus integrates directly into naive resting CD4+ T cells but enters naive cells less efficiently than memory cells. J. Virol. *83*, 4528–4537.

Davis, C.B., Dikic, I., Unutmaz, D., Hill, C.M., Arthos, J., Siani, M.A., Thompson, D.A., Schlessinger, J., and Littman, D.R. (1997). Signal transduction due to HIV-1 envelope interactions with chemokine receptors CXCR4 or CCR5. J. Exp. Med. *186*, 1793–1798.

Deng, Y., Zheng, Q., Ketas, T.J., Moore, J.P., and Lu, M. (2007). Protein design of a bacterially expressed HIV-1 gp41 fusion inhibitor. Biochemistry *46*, 4360–4369.

Doms, R.W., and Peiper, S.C. (1997). Unwelcomed guests with master keys: how HIV uses chemokine receptors for cellular entry. Virology *235*, 179–190.

Elliott, J.I., Surprenant, A., Marelli-Berg, F.M., Cooper, J.C., Cassady-Cain, R.L., Wooding, C., Linton, K., Alexander, D.R., and Higgins, C.F. (2005). Membrane phosphatidylserine distribution as a non-apoptotic signalling mechanism in lymphocytes. Nat. Cell Biol. *7*, 808–816.

Fadeel, B., and Xue, D. (2009). The ins and outs of phospholipid asymmetry in the plasma membrane: roles in health and disease. Crit. Rev. Biochem. Mol. Biol. *44*, 264–277.

Finkelshtein, D., Werman, A., Novick, D., Barak, S., and Rubinstein, M. (2013). LDL receptor and its family members serve as the cellular receptors for vesicular stomatitis virus. Proc. Natl. Acad. Sci. USA *110*, 7306–7311.

Fischer, K., Voelkl, S., Berger, J., Andreesen, R., Pomorski, T., and Mackensen, A. (2006). Antigen recognition induces phosphatidylserine exposure on the cell surface of human CD8+ T cells. Blood *108*, 4094–4101.

Gallay, P., Stitt, V., Mundy, C., Oettinger, M., and Trono, D. (1996). Role of the karyopherin pathway in human immunodeficiency virus type 1 nuclear import. J. Virol. *70*, 1027–1032.

Gottesman, A., Milazzo, J., and Lazebnik, Y. (2010). V-fusion: a convenient, nontoxic method for cell fusion. Biotechniques *49*, 747–750.

Grivel, J.C., and Margolis, L. (2009). Use of human tissue explants to study human infectious agents. Nat. Protoc. *4*, 256–269.

Hammonds, J., Chen, X., Zhang, X., Lee, F., and Spearman, P. (2007). Advances in methods for the production, purification, and characterization of HIV-1 Gag-Env pseudovirion vaccines. Vaccine *25*, 8036–8048.

Harmon, B., and Ratner, L. (2008). Induction of the Galpha(q) signaling cascade by the human immunodeficiency virus envelope is required for virus entry. J. Virol. *82*, 9191–9205.

Harmon, B., Campbell, N., and Ratner, L. (2010). Role of Abl kinase and the Wave2 signaling complex in HIV-1 entry at a post-hemifusion step. PLoS Pathog. *6*, e1000956.

Hendrix, C.W., Flexner, C., MacFarland, R.T., Giandomenico, C., Fuchs, E.J., Redpath, E., Bridger, G., and Henson, G.W. (2000). Pharmacokinetics and safety of AMD-3100, a novel antagonist of the CXCR-4 chemokine receptor, in human volunteers. Antimicrob. Agents Chemother. *44*, 1667–1673.

Kondru, R., Zhang, J., Ji, C., Mirzadegan, T., Rotstein, D., Sankuratri, S., and Dioszegi, M. (2008). Molecular interactions of CCR5 with major classes of small-molecule anti-HIV CCR5 antagonists. Mol. Pharmacol. *73*, 789–800.

Kwong, P.D., Wyatt, R., Sattentau, Q.J., Sodroski, J., and Hendrickson, W.A. (2000). Oligomeric modeling and electrostatic analysis of the gp120 envelope glycoprotein of human immunodeficiency virus. J. Virol. *74*, 1961–1972.

Lackner, A.A., Lederman, M.M., and Rodriguez, B. (2012). HIV pathogenesis: the host. Cold Spring Harb. Perspect. Med. *2*, a007005.

Larsen, C.E., Nir, S., Alford, D.R., Jennings, M., Lee, K.D., and Düzgüneş, N. (1993). Human immunodeficiency virus type 1 (HIV-1) fusion with model membranes: kinetic analysis and the role of lipid composition, pH and divalent cations. Biochim. Biophys. Acta *1147*, 223–236.

Lenz, O., Dittmar, M.T., Wagner, A., Ferko, B., Vorauer-Uhl, K., Stiegler, G., and Weissenhorn, W. (2005). Trimeric membrane-anchored gp41 inhibits HIV membrane fusion. J. Biol. Chem. *280*, 4095–4101.

Malavia, N.K., Zurakowski, D., Schroeder, A., Princiotto, A.M., Laury, A.R., Barash, H.E., Sodroski, J., Langer, R., Madani, N., and Kohane, D.S. (2011). Liposomes for HIV prophylaxis. Biomaterials *32*, 8663–8668.

Matos, P.M., Marin, M., Ahn, B., Lam, W., Santos, N.C., and Melikyan, G.B. (2013). Anionic lipids are required for vesicular stomatitis virus G protein-mediated single particle fusion with supported lipid bilayers. J. Biol. Chem. *288*, 12416–12425.

Melar, M., Ott, D.E., and Hope, T.J. (2007). Physiological levels of virion-associated human immunodeficiency virus type 1 envelope induce coreceptor-dependent calcium flux. J. Virol. *81*, 1773–1785.

Melikyan, G.B. (2008). Common principles and intermediates of viral protein-mediated fusion: the HIV-1 paradigm. Retrovirology *5*, 111.

Miyauchi, K., Kim, Y., Latinovic, O., Morozov, V., and Melikyan, G.B. (2009). HIV enters cells via endocytosis and dynamin-dependent fusion with endosomes. Cell *137*, 433–444.

Morcock, D.R., Thomas, J.A., Gagliardi, T.D., Gorelick, R.J., Roser, J.D., Chertova, E.N., Bess, J.W., Jr., Ott, D.E., Sattentau, Q.J., Frank, I., et al. (2005). Elimination of retroviral infectivity by N-ethylmaleimide with preservation of functional envelope glycoproteins. J. Virol. *79*, 1533–1542.

Otzen, D.E., Blans, K., Wang, H., Gilbert, G.E., and Rasmussen, J.T. (2012). Lactadherin binds to phosphatidylserine-containing vesicles in a two-step mechanism sensitive to vesicle size and composition. Biochim. Biophys. Acta *1818*, 1019–1027.

Pietzsch, J., Gruell, H., Bournazos, S., Donovan, B.M., Klein, F., Diskin, R., Seaman, M.S., Bjorkman, P.J., Ravetch, J.V., Ploss, A., and Nussenzweig, M.C. (2012). A mouse model for HIV-1 entry. Proc. Natl. Acad. Sci. USA *109*, 15859–15864.

Ping, L.H., Joseph, S.B., Anderson, J.A., Abrahams, M.R., Salazar-Gonzalez, J.F., Kincer, L.P., Treurnicht, F.K., Arney, L., Ojeda, S., Zhang, M., et al.; CAPRISA Acute Infection Study and the Center for HIV-AIDS Vaccine Immunology Consortium (2013). Comparison of viral Env proteins from acute and chronic infections with subtype C human immunodeficiency virus type 1 identifies differences in glycosylation and CCR5 utilization and suggests a new strategy for immunogen design. J. Virol. *87*, 7218–7233.

Platt, E.J., Wehrly, K., Kuhmann, S.E., Chesebro, B., and Kabat, D. (1998). Effects of CCR5 and CD4 cell surface concentrations on infections by macrophagetropic isolates of human immunodeficiency virus type 1. J. Virol. *72*, 2855–2864.

Platt, E.J., Durnin, J.P., and Kabat, D. (2005). Kinetic factors control efficiencies of cell entry, efficacies of entry inhibitors, and mechanisms of adaptation of human immunodeficiency virus. J. Virol. *79*, 4347–4356.

Platt, E.J., Bilska, M., Kozak, S.L., Kabat, D., and Montefiori, D.C. (2009). Evidence that ecotropic murine leukemia virus contamination in TZM-bl cells does not affect the outcome of neutralizing antibody assays with human immunodeficiency virus type 1. J. Virol. *83*, 8289–8292.

Platt, E.J., Kozak, S.L., Durnin, J.P., Hope, T.J., and Kabat, D. (2010). Rapid dissociation of HIV-1 from cultured cells severely limits infectivity assays, causes the inactivation ascribed to entry inhibitors, and masks the inherently high level of infectivity of virions. J. Virol. *84*, 3106–3110.

Pleskoff, O., Tréboute, C., Brelot, A., Heveker, N., Seman, M., and Alizon, M. (1997). Identification of a chemokine receptor encoded by human cytomegalovirus as a cofactor for HIV-1 entry. Science *276*, 1874–1878.

Robert, V., Triffaux, E., Savignac, M., and Pelletier, L. (2013). Singularities of calcium signaling in effector T-lymphocytes. Biochim. Biophys. Acta *1833*, 1595–1602.

Scherbik, S.V., and Brinton, M.A. (2010). Virus-induced Ca2+ influx extends survival of west nile virus-infected cells. J. Virol. *84*, 8721–8731.

Segawa, K., Suzuki, J., and Nagata, S. (2011). Constitutive exposure of phosphatidylserine on viable cells. Proc. Natl. Acad. Sci. USA *108*, 19246–19251.

Shao, C., Novakovic, V.A., Head, J.F., Seaton, B.A., and Gilbert, G.E. (2008). Crystal structure of lactadherin C2 domain at 1.7A resolution with mutational and computational analyses of its membrane-binding motif. J. Biol. Chem. *283*, 7230–7241.

Shaw, G.M., and Hunter, E. (2012). HIV transmission. Cold Spring Harb. Perspect. Med. *2*, 2.

Suzuki, J., Umeda, M., Sims, P.J., and Nagata, S. (2010). Calcium-dependent phospholipid scrambling by TMEM16F. Nature *468*, 834–838.

Weissenhorn, W., Dessen, A., Harrison, S.C., Skehel, J.J., and Wiley, D.C. (1997). Atomic structure of the ectodomain from HIV-1 gp41. Nature *387*, 426–430.

Wilen, C.B., Tilton, J.C., and Doms, R.W. (2012). HIV: cell binding and entry. Cold Spring Harb. Perspect. Med. *2*, 2.

Wu, Y., and Yoder, A. (2009). Chemokine coreceptor signaling in HIV-1 infection and pathogenesis. PLoS Pathog. *5*, e1000520.

Zaitseva, E., Yang, S.-T., Melikov, K., Pourmal, S., and Chernomordik, L.V. (2010). Dengue virus ensures its fusion in late endosomes using compartment-specific lipids. PLoS Pathog. *6*, e1001131.

Zhao, F., Li, P., Chen, S.R., Louis, C.F., and Fruen, B.R. (2001). Dantrolene inhibition of ryanodine receptor Ca2+ release channels. Molecular mechanism and isoform selectivity. J. Biol. Chem. *276*, 13810–13816.

STAR★METHODS

KEY RESOURCES TABLE

REAGENT or RESOURCE	SOURCE	IDENTIFIER
Antibodies		
Human CD4 monoclonal antibody (Sim.4)	AIDS Reagent Program, NIAID, NIH; https://www.aidsreagent.org/	#724
CCR5 monoclonal antibody	AIDS Reagent Program, NIAID, NIH; https://www.aidsreagent.org/	#45549
CXCR4 Monoclonal Antibody (12G5)	AIDS Reagent Program, NIAID, NIH; https://www.aidsreagent.org/	#3439
Bacterial and Virus Strains		
HIV-$1_{LAI.04}$	Virology Quality Assurance Laboratory; Rush Presbyterian/St. Luke's Medical Center, Chicago, IL; this study	N/A
Biological Samples		
Human tonsillar tissues	Children's National Medical Center (Washington, DC); https://childrensnational.org/	N/A
Chemicals, Peptides, and Recombinant Proteins		
CCR5 Inhibitor TAK-779	AIDS Reagent Program, NIAID, NIH https://www.aidsreagent.org	#4983
CXCR4 Inhibitor AMD-3100	AIDS Reagent Program, NIAID, NIH https://www.aidsreagent.org	#8128
C52L recombinant peptide	Gift from Dr. Min Lu, University of New Jersey, New Brunswick, NJ); Deng et al., 2007	N/A
HIV-1 JR-FL gp140CF recombinant protein	AIDS Reagent Program, NIAID, NIH https://www.aidsreagent.org	Cat# 12573
Recombinant protein HIV-1 IIIB gp120	AIDS Reagent Program, NIAID, NIH https://www.aidsreagent.org	Cat #11784
CaCCinh-A01	Tocris, Minneapolis,MN	#4877 cas# 407587-33-1 lot 1B191479
BAPTA AM	Cayman Chemical, MI	#15551 CAS # 126150-97-8
thapsigargin	Cayman Chemical, MI	# 10522 CAS #67526-95-8
cyclopiazonic acid	Cayman Chemical, MI	#11326 CAS #18172-33-3
Hexadimethrine bromide	Sigma-Aldrich, MO	#107689 CAS #
CCF4-AM	Invitrogen Carlsbad,CA	#K1029 lot#1642430A
16:0-06:0 NBD PS	Avanti Polar Lipids, AL	#810192 CAS# 384833-06-1
16:0-06:0 NBD PC	Avanti Polar Lipids, AL	#810130 CAS # 91992-01-7
16:0-06:0 NBD PG	Avanti Polar Lipids, AL	#810163 CAS # 474942-85-3
LPC	Avanti Polar Lipids, AL	#855475 CAS #20559-18-6
Vybrant DiI	Molecular Probes, OR	#V22885 lot#1241506
Hoechst 33342	Molecular Probes, OR	#62249 ND1539391
DAPI	Molecular Probes, OR	#62247 CAS # 1H-Indole-6-carboximidamide

(*Continued on next page*)

Continued

REAGENT or RESOURCE	SOURCE	IDENTIFIER
Experimental Models: Cell Lines		
HEK293T/17	ATCC, Manassas, VA	#ACS-4500
HeLa (CCL-2)	ATCC, Manassas, VA	#CCL-2
TZM-bl cells	AIDS Reagent Program, NIAID, NIH; Platt et al., 1998	#8129
JC.10 cells	Dr. D. Kabat (OHSU,OR); Platt et al., 1998	N/A
HeLa-ADA	Dr. M. Alizon (Pasteur Institute, France); Pleskoff et al., 1997	N/A
TF228.1.16 cells	AIDS Reagent Program, NIAID, NIH	Cat# 11481
U87.CD4.CCR5	AIDS Reagent Program, NIAID, NIH	Cat# 4035
Jurkat-Tat-CCR5	Quentin Sattentau (University of Oxford, UK); Morcock et al., 2005	N/A
DEIR PIV	Dr. Yuri Lazebnik (CSHL); Gottesman et al., 2010	N/A
HeLa-ADA/eGFP	This paper	N/A
HeLa ADA/RFP	This paper	N/A
TZM-bl/eGFP	This paper	N/A
TZM-bl/RFP	This paper	N/A
TF228.1.16 /RFP	This paper	N/A
HeLa4 cells	This paper	N/A
HeLa45	This paper	N/A
HeLa45wt	This paper	N/A
HeLa45const.	This paper	N/A
HeLa45sh	This paper	N/A
HeLa45control sh	This paper	N/A
HeLa45shwtR	This paper	N/A
Jurkat-Tat-CCR5/A901	This paper	N/A
Jurkat-Tat-CCR5/C112	This paper	N/A
Oligonucleotides		
For TMEM16Fh(shR): ATT GCA GCC AAG CTG GCT CTT ATC ATT GTC	This paper	N/A
For TMEM16Fh shRNA: TTGCAGCCAAGC TGGCTCTTATCATTGTC	Origene, MD	HuSH pRFP-C-RS
For control shRNA: GCACTACCAGAGCT AACTCAGATAGTACT	Origene, MD	HuSH pRFP-C-RS-control
Recombinant DNA		
All plasmid constructs used in this study are listed in the Table S1	This paper	N/A
Software and Algorithms		
Sigmaplot v.13.0	Systat Software, San Jose, CA	N/A
Fiji: an open-source platform for biological-image analysis	http://fiji.sc/	N/A

CONTACT FOR REAGENT AND RESOURCE SHARING

Further information and requests for resources and reagents should be directed to and will be fulfilled by the Lead Contact, Leonid Chernomordik (chernoml@mail@mail.nih.gov).

EXPERIMENTAL MODEL AND SUBJECT DETAILS

Human tonsillar tissue model was described in details elsewere (Grivel and Margolis, 2009). Briefly, human tonsils were obtained from routine tonsillectomy (unrelated to the current study) performed in the Children's Hospital (Washington, DC). Tissues were received

from the Pathology Department and were considered as ''pathological waste.'' Tissue samples were anonymized and the protocol was approved by the NIH Office of Human Subject Research (NIH-OHSRP-00099). Tissues were dissected into ~2mm blocks, and incubated at the air/liquid interface on collagen sponges (9 blocks per sponge) in 6-well plates supplemented with RPMI 15% FBS (18 blocks of tissue per condition).

Cells

HEK293T/17 and HeLa (CCL-2) cells were purchased from American Type Culture Collection (ATCC), Manassas, VA. HeLa-derived TZM-bl cells expressing CD4, CXCR4, and CCR5 (Platt et al., 1998) (donated by Drs. J.C. Kappes and X. Wu) were obtained from the NIH AIDS Research and Reference Reagent Program. HeLa-derived JC.10 cells, which stably express large amounts of CD4 and low amounts of CCR5 (Platt et al., 1998), were a generous gift from Dr. D. Kabat (OHSU, OR). HeLa-ADA cells stably expressing Env and Tat from the HIV-1 ADA strain were a kind gift from Dr. Marc Alizon (Pasteur Institute, France). TF228.1.16 cells (B cell lymphoma) modified to stably express the entire HIV-1 (BH10-X4 tropic) envelope protein gp160 were obtained through the NIH AIDS Reagent Program, NIAID, NIH. TF228.1.16 cells were obtained from Drs. Zdenka Jonak and Steve Trulli. U87.CD4.CCR5 - human astrocytoma (glioblastoma) cells that express CD4 and CCR5 were obtained from Dr. HongKui Deng and Dr. Dan R. Littman through the NIH AIDS Reagent Program.

Jurkat-Tat-CCR5 cells (JkT-CCR5), a T cell line that has been transfected with the HIV-1 *tat* gene and the CCR5 coreceptor (Morcock et al., 2005) to render it permissive to X4 and R5 viruses, were kindly provided by Quentin Sattentau (Sir William Dunn School of Pathology, University of Oxford, Oxford, United Kingdom).

For this study we have developed the following cell lines: (1) HeLa-ADA/eGFP cells (= HeLa-ADA cells stably expressing eGFP), (2) HeLa ADA/RFP (= HeLa-ADA cells stably expressing mCherry), (3) TZM-bl/eGFP (= TZM-bl cells stably expressing eGFP), (4) TZM-bl/RFP (= TZM-bl cells stably expressing mCherry), and (5) TF228.1.16 /RFP cells (= cells stably expressing mCherry). Based on HeLa (CCL-2) cells, we also developed (6) HeLa4 cells (= HeLa cells expressing CD4), (7) HeLa45 (= HeLa cells expressing CD4 and CCR5), (8) HeLa45wt (= HeLa45 cells expressing wild-type hTMEM16F –Clover), (9) HeLa45const. (= HeLa45 cells expressing constitutively active D409G mutant of hTMEM16F-Clover), (10) HeLa45sh (= HeLa45 cells expressing TMEM16F shRNA), (11) HeLa45shwtR (= HeLa45sh cells expressing hTMEM16F resistant to aforementioned shRNA-Clover), and (12) HeLa45control sh (= HeLa45 cells expressing control shRNA). Note that we have developed and characterized two clones of HeLa45wt (clones 4 and 9). In the experiments presented in Figures S4C and S4D we used the cells of both clones and in all other experiments (Figures 1, 3, 6 and S3) we used only HeLa45wt cells of clone 4.

Based on JkT-CCR5 cells, we developed (13) A901 cells (= JkT-CCR5 cells expressing TMEM16F shRNA), and (14) C112 cells (= JkT-CCR5 cells expressing control (non-target) shRNA).

Cell lines expressing cloned genes were produced by lentiviral transduction using LeGo pseudoviruses with corresponding encoding genes. These pseudoviruses were produced by co-transfecting HEK293T cells in 10 cm dishes with 10 μg of psPAX2, 10 μg of plasmid encoding genes of interest, and 10 μg of pMD2.G vector expressing VSV G. Pseudoviruses were added to the cells in a medium containing 7-μg/ml hexadimethrine bromide and incubated at 37°C for 3 days. Cells were detached and plated at a low density in the presence of corresponding antibiotics for the selection and for the subsequent cloning by a limited dilution.

JkT-CCR5 cells with TMEM16F activity suppressed by shRNA and cells expressing control shRNA (A901 and C112 cells) were produced by transduction with lentiviruses encoding either TMEM16F shRNA-Clover-BSD or control shRNA-Clover-BSD. Three days after lentiviral transduction, we sorted the bright green fluorescent viable cells using BD FACSARIA Fusion Cell Sorter and maintained them in the presence of 30-μg/ml of Blasticidin. Because of unstable expression of shRNA, cells were not used after seven passages.

HeLa45sh and HeLa45control sh cells were produced by lentiviral transduction of the HuSH pRFP-C-RS plasmid vector encoding a TMEM16Fh shRNA and the HuSH pRFP-C-RS plasmid vector encoding a control shRNA. The cells were selected with 3-μg/ml of Puromycin for 5 days. The cells were used, without cloning, for fewer than seven passages.

HEK293T cells, and HeLa cells, and their derivatives, were grown in Dulbecco's Modified Eagle high glucose medium (DMEM) (GIBCO, Madison, WI). JkT-CCR5 cells, their derivatives, and TF228.1.16 cells were grown in RPMI-1640 (GIBCO) supplemented with 10% fetal bovine serum (FBS, HyClone Laboratories, Logan, UT) and 25 mM HEPES (pH 7.5) at 37°C and 5% CO_2.

DEIR PIV cells expressing VSV G and RFP (Gottesman et al., 2010), a kind gift from Dr. Yuri Lazebnik (Cold Spring Harbor Laboratory), were grown in Dulbecco's Modified Eagle high glucose medium (DMEM) with 10% FBS.

Pseudoviruses

We produced pseudoviruses by transfecting HEK293T cells in 10-cm dishes using the ViaFect Transfection Reagent (Promega Co. Madison, WI). The fluorescently labeled pseudoviruses were produced by co-transfecting 10 μg of psPAX2, 10 μg of Gag-Ruby2 or Gag-Clover, and 10 μg of pCAGGS encoding JR-FL or HXB2 HIV-1-Env expression vector. Infectious titer of our pseudovirus preparations was measured on the cells used in the particular experiments (TZM-bl or JkT-CCR5 or U87.CD4.CCR5). MOI of ~0.5 for 10^4 cells corresponded to ~0. 4 ng p24/ml for JR-FL or BAL.01; 2.7 ng p24/ml for HXB2 and ~6 ng p24/ml for JR-CSF. p24 was measured with a dynamic immunofluorescent cytometric bead assay (Biancotto et al., 2009).

To quantify single-round infection, we used LeGo-T2 pseudoviruses encoding a tandem dimer of Tomato fluorescent reporter protein. These pseudoviruses were produced by co-transfecting HEK293T cells with 10 μg of psPAX2, 10 μg of LeGo-T2 and 10 μg of HIV1-Env expression vector. The virus-containing medium was harvested at 48 hr post-transfection and passed through a 0.45-μm filter.

In the virus–cell fusion experiments, we used pseudoviruses containing the β-lactamase-Vpr (BlaM-Vpr). HIV-1 pseudoviruses bearing HXB2, JR-CSF or VSV-G envelope glycoproteins and the β-lactamase-Vpr chimera (BlaM-Vpr) were produced by co-transfecting HEK293T/17 cells in a 10-cm dish with 2 μg of the HIV-based pR8ΔEnv packaging vector, 2 μg of pMM310, 1 μg of pcRev, and 3 μg of vector encoding envelope glycoprotein, using the jetPRIME® transfection reagent (Polyplus Transfection, Illkirch-Graffenstaden, France). The transfection medium was replaced with fresh DMEM/10% FBS after 12ch, and cells were cultured for 36ch, after which the virus-containing culture medium was collected, passed through a 0.45-μm filter, aliquoted, and stored at −80°C. Infectious titers were determined with a β-Gal assay, using TZM-bl cells. The p24 amount of pseudoviruses was determined by p24 antigen capture ELISA, as described in (Hammonds et al., 2007). Briefly, the 96-well plate (Thermo Scientific, MA) was coated overnight at 37 C with the anti-p24 antibody 183-H12-5C (CA183 from Bruce Chesebro and Kathy Wehrly) obtained through the NIH AIDS Reagent Program. The wells were blocked for 1 hr at 37 C with 5% heat-inactivated fetal bovine serum in PBS. Diluted pseudoviruses in p24 sample diluent (10% heat-inactivated fetal bovine serum, 0.5% Triton X-100 in PBS) were applied to CA183-coated plates for 2h at 37 C. The bound p24 was determined using HIV-Ig (NABI, NIH AIDS Reagent Program) for 1h at 37 C, followed by incubation with HRP-conjugated goat anti-human (Thermo Scientific, MA) for 1h at 37 C. Colorimetric analysis was performed using TMB substrate (Thermo Scientific, MA) and absorbance was read at 450nm on SpectraMaxi3 fluorescence plate reader (Molecular Devices, CA). Recombinant p24 was used for the standard curve.

Viruses

CXCR4-tropic LAI.04 (HIV-$1_{LAI.04}$) (50 ng p24/ml) were produced in peripheral blood mononuclear cells by the Virology Quality Assurance Laboratory (VQA; Rush Presbyterian/St. Luke's Medical Center, Chicago, IL).

METHOD DETAILS

Reagents

TAK-779 (Kondru et al., 2008), and AMD-3100 (Hendrix et al., 2000) were obtained through the NIH AIDS Reagent Program, NIAID, NIH. The C52L recombinant peptide derived from the HIV-1 gp41 glycoprotein was a generous gift from Dr. Min Lu (University of New Jersey, New Brunswick, NJ).

R5-tropic HIV-1 JR-FL gp140CF recombinant protein (Cat# 12573), from Duke Human Vaccine Institute, Duke University Medical Center; and X4-tropic recombinant HIV-1 IIIB gp120 (CHO) (Cat #11784), produced by ImmunoDX, LLC, were obtained through the NIH AIDS Reagent Program, NIAID, NIH.

CaCCinh-A01 was purchased either from EMD Millipore Billerica, MA or from Tocris, Minneapolis, MN. Most of this study has been carried out with CaCCinh-A01 purchased from Calbiochem (Cat # 208293; Lot: D00130825). At the time of the revision of the paper, we again purchased CaCCinh-A01 from Calbiochem (now part of MilliporeSigma), Cat # 208293, lot: D00160869. We found A01 of this new lot to be too toxic for the cells to achieve fusion- and infection- inhibiting concentrations. HPLC and mass spectroscopy revealed significant amounts of impurities in this reagent. We have shifted to CaCCinh-A01 from Tocris (Cat. No. #4877, Batch No.: 2, # 1B191479) and found no impurities in this reagent. The reagent had low toxicity and was used in the experiments presented in Figures 5A, 5B, and 6E, and Figures S5B–S5D.

BAPTA acetoxymethyl ester (BAPTA AM), thapsigargin (Tg), cyclopiazonic acid (CPA), and dantrolene were purchased from Cayman Chemical, Ann Arbor, MI. Hexadimethrine bromide and Cellstripper were purchased from Sigma-Aldrich, St. Louis, MO and from Corning, Manassas, VA, respectively. CCF4-AM was obtained from Invitrogen (Carlsbad, CA).

Human CD4 monoclonal antibody (Sim.4) from Dr. James Hildreth, CCR5 monoclonal antibody (#45549), and CXCR4 Monoclonal Antibody (12G5 from Dr. James Hoxie) were obtained through the NIH AIDS Reagent Program, NIAID, NIH.

All the lipids used in this study: 16:0-06:0 NBD PS (1-palmitoyl-2-{6-[(7-nitro-2-1,3-benzoxadiazol-4-yl)amino]hexanoyl}-*sn*-glycero-3-phosphoserine), 16:0-06:0 NBD PC (1-palmitoyl-2-{6-[(7-nitro-2-1,3-benzoxadiazol-4-yl)amino]hexanoyl}-*sn*-glycero-3-phosphocholine), 16:0-06:0 NBD PG (1-palmitoyl-2-{6-[(7-nitro-2-1,3-benzoxadiazol-4-yl)amino]hexanoyl}-*sn*-glycero-3-[phospho-*rac*-(1-glycerol)])), and LPC (1-*lauroyl*-2-hydroxy-sn-glycero-3-phosphocholine) were purchased from Avanti Polar Lipids, Alabaster, AL. The fluorescent lipophilic tracer Vybrant DiI (#V22885), Hoechst 33342 (#62249), and DAPI (#62247) were purchased from Molecular Probes Inc., Eugene, OR.

Plasmid Constructs

All plasmid constructs used in this study are listed in Table S1. Plasmids developed for this work were constructed according to standard molecular biology methods, including PCR using Q5 polymerase (NEB, MA), overlap extension PCR, restriction fragment ligation, and In-Fusion cloning (Clontech, CA). All constructs were sequence verified. Complete plasmid sequences are available upon request.

Clover-LactC2 Purification

A cDNA construct consisting of Clover fluorescent protein followed by a hexa-histidine tag and lactadherin-C2 (Clover-$(His)_6$-LactC2) in the pET-28 bacterial expression vector together with pLysSRARE2 plasmid (Novogen, WI) were electroporated into CleenColi BL21(DE3) according to manufacturer protocol (Lucigen, WI). Lactaherin is also known as MFGE8, HGNC:7036). Cells were grown in TB medium at 37°C in 50-μg/ml kanamycin and 30-μg/ml chloramphenicol until the culture reached $A_{600} = 1$. After addition of 1 mM IPTG, the culture was grown for 3 hr at 28°C. Cells were lysed in B-Per (Thermo Scientific, MA) containing benzonase and protease inhibitor cocktail III (Calbiochem, CA). After centrifugation at 20,000 × *g* for 20 min, Clover-$(His)_6$-LactC2 was purified from the supernatant on a 1 mL cOmplete His-Tag Purification affinity column (Roche, CA). Stock solutions of 1–3 mg/ml were stored in the elution buffer (250 mM imidazole, pH 8.0) and were used at ?1–3 μg/ml. LactC2 and LactC2-Ruby2 were purified similarly.

Virus Binding

To quantify virus-to-cell binding, we incubated cells with fluorescent (Gag-clover) viruses pseudotyped with JR-FL Env (38 ng p24/ml; 10^4 cells in 100 μl)) at 22°C for 45 min in the full medium with 7-μg/ml hexadimethrine bromide. Using fluorescence microscopy, we selected the amount of virus to apply to get ~20 fluorescently labeled cell-associated particles per cell on average. Unbound viruses were washed out, and cells were imaged with the C-Apochromat 40x/1.2 W objective on the Zeiss LSM510 confocal microscope. For each condition we analyzed at least seven fields of view.

PS Externalization Assay

We quantified the PS content in the outer leaflet of the plasma membrane using LactC2-tagged with either Ruby or Clover fluorescent proteins. The cells in ibidi-treated μ-Dish (35 mm) (ibidi (#81156)) or, for suspension cells, in uncoated μ-Slides (ibidi (#81501)) were incubated with mock solutions or gp120 or pseudoviruses (~38 ng p24/ml; 10^4 cells in 100 μl) at 22°C for 15 min. Using fluorescence microscopy, we selected the amount of virus to apply to get ~20 fluorescently labeled cell-associated particles per cell on average. Then, fluorescent LactC2 was added, to a final concentration of 100 nM. If not stated otherwise, cell-surface associated LactC2 was imaged 45 min after its application. The cells were imaged with the C-Apochromat 40x/1.2 W objective on the Zeiss LSM510 confocal microscope to acquire confocal z stacks. To quantify PS externalization, fluorescent signal in all slices was summed and normalized by the surface area occupied by cells in each frame. Regions with dead cells were manually identified in bright field channel and excluded from analysis. We analyzed 6 to 36 fields per experimental condition using open-source software ImageJ Fiji (http://fiji.sc/).

Cell-Cell Fusion

We quantified cell–cell fusion using several assays. (1) In the first assay, referred to as *fusion per contact*, we used Env cells stably expressing EGFP and target cells expressing mRedFP. We detached cells using Cellstripper and co–plated them at a 1:1 ratio in 96 well plates. After a 45 min incubation at 22°C, the cells were incubated at 37°C for 1 hr before imaging using a Zeiss Observer Z1 fluorescence microscope. The average number of co-labeled cells per field of view was normalized to the average number of contacts between differently labeled cells in the control experiment without warming up to 37°C. (2) In the second assay, referred to as *fusion per target cell*, Env cells expressing eGFP cells were seeded in 96-well plates to achieve next-day 85%–90% confluence. We detached target/RFP cells using Cellstripper and added 200–250 target/RFP cells to each well with Env/eGFP cells. After incubation at 22°C for 45 min, unbound cells were removed and the temperature was raised to 37°C. The cells were imaged 1 hr later. The number of co-labeled cells was normalized to the number of the target cells added to each well. In case of JC10 cells and TF228.1.16 cells the cells were preincubated with Env cells and TZM-bl cells, respectively, at 22°C for 3 hr instead of 45 min. The temperature was raised to 37°C for 4 hr before imaging. The number of multinuclear co-labeled cells was calculated in each well. This assay is a variation on a well-known 'fusion from without' assay in which two target cells fuse via cell-bound virions. Two differently labeled Env-expressing cells do not fuse with each other because neither of the cells expresses CD4 and coreceptors. However, in our assay, fusion of each of these cells to unlabeled target cell generates double-labeled cell and presents the measure of the ability of these target cells to support Env-mediated fusion.

Hemifusion

To assay cell–cell hemifusion, we modified the *fusion per target cell* assay. The detached RFP-expressing Env cells were labeled with the fluorescent lipophilic tracer Vybrant DiI (2μM final) in the medium without serum for 15 min at room temperature, washed with full medium and added to the monolayer of unlabeled TZM-bl cells labeled with Hoechst 33342 (1μg/ml) and incubated as above. After incubation at 22°C for 45 min, unbound cells were removed and the temperature was raised to 37°C. The cells were imaged 1 hr later to count attached TZM-bl cells labeled with both RFP and DiI (content mixing) or only DiI (hemifusion). Numbers of membrane probe– or content probe–labeled target cells were normalized to the number of the Env cells in the field of view.

Virus–Cell Fusion

TZM-bl cells ($0.5 \cdot 10^5$ cells/well) were seeded into a Costar black clear-bottom 96-well plate (Corning, New York, NY) in growth phenol red-free medium the day before the experiment. We measured virus–cell fusion with JkT-CCR5 cells in suspension by

dispensing $1.5 \cdot 10^5$ cells/well in 96-well U-bottom plates (Corning). Viruses were added to cells at a multiplicity of infection (MOI) of ?1 for TZM-bl cells and ~3 for JkT-CCR5-based cells (10 ng p24/ml for HXB2 and VSV-G and 12 ng p24/ml for JR-CSF for 10^5 cells in 50 μl); and centrifuged at 1,550 × g for 30 min at 4°C.

For A01 inhibition experiments, TZM-bl were pretreated for 30 min at 37°C, 5% CO_2 with varied concentrations of compound diluted in medium lacking phenol red and FBS. Inhibitor was removed, and pseudoviruses were bound to adherent TZM-bl cells by centrifugation at 1,550 × g for 30 min at 4°C. Cells were washed and incubated for 90 min at 37°C, 5%CO_2, in the absence or presence of the indicated inhibitors in phenol red/FBS-free medium.

Note that virus-cell assay was the only assay in which we used spinoculation. The fusion reaction was stopped by briefly chilling the plates on ice, and cells were loaded with the CCF4-AM substrate. We incubated the cells overnight at 12°C and measured the resulting ratio of blue to green fluorescence emission, which reflected the intracellular β-lactamase activity, using the SpectraMaxi3 fluorescence plate reader (Molecular Devices, CA). Two independent experiments were performed in triplicates. We treated our experimental design as randomized block design and tested statistical significance in SigmaPlot v.13.0 using two-way ANOVA with experiments as additional nominal factor. For presentation we normalized the data points for each out of the two independent experiments, pooled these together (6 points for each condition) and calculated the mean and SEM. We measured cell viability using a colorimetric CellTiter Blue assay (Promega) according to the manufacturer's recommendations.

Single-Round Infection

The HeLa-derived cells were seeded to 96-well plates to form a cell monolayer. In the case of JkT-CCR5-based cells, we placed $2x10^4$ cells in each well in the serum-free medium. Serial dilutions of LeGo-T2 pseudoviruses encoding a tandem dimer of Tomato (tdTomato) fluorescent reporter protein (X4-tropic HXB2 at MOI of 0.5 (2.7 ng p24/ml), and R5-tropic JR-FL at MOI of 0.5 (0.4 ng p24/ml), BaL.01 at MOI of 0.5 (0.44 ng p24/ml) and JR-CSF at MOI of 0.5 (6 ng p24/ml) were added to the cells in triplicates and incubated for 2 hr at 22°C. Then the temperature was raised to 37°C for 5 hr. After that, 10% serum was added to each well and plates were incubated for 72 hr at 37°C. We quantified infection by scoring the number of Tomato-labeled cells using fluorescence microscopy. Due to recombinational instability of the tdTomato, this assay strongly understates infection, as evidenced by an experiment in which we compared the levels of infection in U87.CD4.CCR5 cells scored for JR-CSF pseudotyped LeGo viruses at MOI of 0.5 (6 ng p24/ml; 10^4 cells in 100 μl) encoding the tdTomato with those observed for the JR-CSF pseudotyped PNL4.3-Clover viruses at MOI of 0.5 (5 ng p24/ml; 10^4 cells in 100 μl) (Figure S6B). For viruses with different reporters produced at exactly same conditions and applied in the same amounts, the mean number of the Tomato-labeled cells/well was 3.8-fold lower than the number of the Clover-labeled cells. However, the normalized data on the dose dependence of A01 inhibition of the infection for different reporter proteins were practically indistinguishable, confirming the validity of the normalized single round infection assays with tdTomato presented in our study.

Infection with Live Virus

JkT-CCR5 cells were infected as previously described. Briefly, 10^5 cells (in 100μl of medium) were inoculated with 100μl of $HIV_{LAI.04}$ suspension containing 5 ng, 0.5 ng or 0.05 ng of p24. Cells and HIV were incubated for 2 hr at 37°C. Infected cells were washed and transferred to 24-well plates with one 1 mL of culture medium and further cultured for 7 days. Each experimental condition was performed in triplicate. At days 3 or 7, JkT-CCR5 cells were stained with anti-CD4-BV650 and CXCR4-BV421 antibodies purchased from Biolegends. Following surface staining, the cells were permeabilized (FIX &PERM kit, ThermoFisher Scientific) and stained for intracellular p24 with anti-p24-PE (Beckman Coulter) antibodies. Gating strategy used for the flow cytometry analysis of the infection is illustrated in Figure S7. Dead cells were determined and excluded from analysis with the LIVE/DEAD Fixable Blue Dead Cell Stain Kit (Invitrogen). Data was acquired on Flow Cytometer LSR II (BD Biosciences, San Jose, CA) equipped with 355-, 407-, 488-, 532- and 638- nm lasers and analyzed with FlowJo software 10.0.7r2 (Treestar Software, Ashburn, OR).

Human tonsillar tissues were inoculated with 5 μl of $HIV_{LAI.04}$ viral stock (50ng of p24/ml), and treated with A01 at different concentrations. The media collected at days 6, 9 and 12 were pooled together and HIV infection was assessed by measuring p24 release into culture medium with a dynamic immunofluorescent cytometric bead assay (Biancotto et al., 2009). Since CD4 expression is down-regulated in HIV-1 infection, cytotoxic effects of A01 on the cells targeted by HIV-1 were evaluated from measurements of the numbers of live CD45+/CD3+/CD8- cells in the tissue blocks.

We quantified expression of CD4 and CCR5 on live cells with anti-CD4-BV650 (Biolegend) and anti-CCR5 –PeCy7 (BD Pharmigen) antibodies, by converting mean fluorescence intensities to antibody binding capacity (ABC) values using standardized beads (Bangs Laboratories).

VSV G mediated Cell-Cell Fusion

Fusion between DEIR PIV expressing VSV G and RFP co-plated overnight with TZMbl cells expressing GFP was triggered by a 2 min application of acidic media of pH 5.5, 6.0, and 6.2; or, in the control, pH 7.4 medium. Immediately prior to acidic pH application, the cells were treated at 22C° with either 1 μM NBD-PS (5 min at 22C°) or with 200 μM LactC2 for 15 min or left untreated. After low pH application, the cells were returned to pH 7.4 and, after 30min incubation at 37°C. Fusion was detected as appearance of yellow cells (i.e., cells labeled with both RFP and GFP). Fusion extents were quantified by normalizing the number of fused DEIR PIV-RFP/TZMbl –GFP cells to the total number of contacts between DEIR PIV cells and TZMbl cells.

Adding Exogenous Lipids

A stock solution of lauroyl LPC (10mM in water) used to reversibly block fusion was freshly prepared. Contacting Env cells and target cells were placed at 22°C in 100 μM lauroyl LPC-supplemented medium without FBS; 5 min later the temperature was raised to 37°C; 1 hr later, the cells, still at 37°C; were washed with LPC-free complete medium supplemented or not with LactC2, TAK-779, or PS. The images were taken and analyzed 1 hr later.

To incorporate exogenous NBD-labeled lipids (PS, PC, or PG) into plasma membranes of the cells, a 2.5 mM stock solution of PS, PC or PG in ethanol was first diluted to a 50x concentration in water, then diluted by the serum-free medium to 2.5 μM with fast vortexing and lipid-supplemented medium immediately added to the contacting Env cells and target cells. Similar levels of cell-associated NBD fluorescence observed with fluorescence microscopy suggested that PS, PC, and PG partitioned into the cell membranes to similar concentrations. Immediately after application of the lipids at 22°C, the temperature was raised to 37°C, and 1 hr later fusion was scored as described above.

Temperature-Arrested Stage

To establish TAS (Melikyan, 2008), we co-incubated Env cells and TZM-bl cells for 3 hr, at 22°C. As described earlier (Melikyan, 2008), robust fusion after raising of the temperature to 37°C was already insensitive to TAK-779, confirming that fusion downstream of TAS does not depend on additional gp120–CCR5 interactions.

Application of Inhibitors

In the PS externalization assay, coreceptor antagonists TAK-779 and AMD-3100 were added 5 min before application of virus or soluble gp120. In fusion assays, the antagonists and C52L were applied to the contacting Env-expressing cells and target cells 5 min before raising the temperature to 37°C and were present during fusion.

The target cells were incubated for 1 hr at 37°C in medium without FBS with BAPTA AM (10 μM), a membrane-permeable chelator of intracellular calcium (10 μM), thapsigargin (Tg) (2 μM), cyclopiazonic acid (CPA)(10 μM), and dantrolene (100 μM). After washing, the cells were co-plated with Env cells for fusion assays. A01 was applied to contacting Env cells and target cells and was present during fusion.

QUANTIFICATION AND STATISTICAL ANALYSIS

If not stated otherwise, for each condition, we carried out at least 3 independent experiments and analyzed at least 10 microscopic fields in each microscopy experiment. We prepared graphs and performed statistical analyses using Sigmaplot v.13.0 (Systat Software, San Jose, CA). All pairwise comparisons were tested for statistical significance using the unpaired Student's t test or, in case of virus-cell fusion two-way ANOVA (see above). Data are presented as the means ± SEM with the number of experiments *n* stated.

Cell Host & Microbe, Volume *22*

Supplemental Information

Fusion Stage of HIV-1 Entry Depends on Virus-Induced Cell Surface Exposure of Phosphatidylserine

Elena Zaitseva, Eugene Zaitsev, Kamran Melikov, Anush Arakelyan, Mariana Marin, Rafael Villasmil, Leonid B. Margolis, Gregory B. Melikyan, and Leonid V. Chernomordik

Supplemental Information

FUSION STAGE OF HIV-1 ENTRY DEPENDS ON VIRUS-INDUCED CELL SURFACE EXPOSURE OF PHOSPHATIDYLSERINE

Elena Zaitseva, Eugene Zaitsev, Kamran Melikov, Anush Arakelyan, Mariana Marin, Rafael Villasmil, Leonid B. Margolis, Gregory B. Melikyan, Leonid V. Chernomordik

Supplementary legends

Figure S1. Time course of phosphatidylserine exposure after virus application, related to Figure 1. A. In the presence of LactC2-Clover (green), R5-tropic pseudovirus (JR-FL, ~20 virions per cell) was added to JkT-CCR5 cells at t=0 at 22°C. The cells were imaged (fluorescence microscopy at the top and bright field at the bottom) at t=3, 6, 13, 23, and 33 min after virus application. The images on the right – control, in which viral suspension was replaced with mock solution, at t =33 min. **B**. Quantification of images such as those in **A**. LactC2 fluorescence at each time point is normalized to that at t=33 min after virus application. **C.** Cumulative distribution function of overall LactC2 fluorescence in single cells at t=33 min.

Figure S2. Binding of soluble gp120 to the JkT-CCR5 cells induces PS exposure at the cell surface, related to Figure 1. PS exposure at the surface of JkT-CCR5 cells, which express CD4 and both CXCR4 and CCR5 coreceptors, was detected as labeling with LactC2-Clover (green). The cells were incubated with 20 nM soluble recombinant gp120 either of R5-tropic JR-FL strain (images 2, 4, 6 and 8) or X4-tropic HIV-1 IIIB strain (images 3, 5, 7, and 9). Image (1) Control without gp120 application. Images (4, 5) 2μM TAK-779; (6,7) 2μM AMD-3100; (8,9) 60 μM A01. Representative fluorescence microscopy images were taken 1 h after gp120 application.

Figure S3. The dependence of virus-induced PS externalization on TMEM16F expression, related to Figure 1. Representative fluorescence and bright field images for the experiments presented in Figure 1C. R5-tropic pseudovirus (JR-FL) was added at 22°C to HeLa 45 cells with modified expression of TMEM16F in the presence of LactC2-Ruby (red). Cell surface PS (=LactC2 labeling) 1 h after virus application (lower panel, 1B-5B) and without it (upper panel, 1A-5A) for HeLa45 cells expressing control shRNA (1), TMEM16F-silencing shRNA (2) and TMEM16F-silencing shRNA together with an shRNA-resistant form of the TMEM16F protein (3). (4) and (5) HeLa45 cells overexpressing w.t. TMEM16F (4) and constitutively active mutant TMEM16F (5).

Figure S4. Promotion of cell fusion mediated by X4-tropic Env (A) and for the target cells with a low surface concentration of coreceptors (B) by exogenous PS; CD4 and CCR5 expression in the cells with modified TMEM16F expression (C, D); and placing the PS-dependent stage before the LPC-arrested fusion stage (E), related to Figures 2 (A,B), 3 (C,D) and 4 (E). A. Exogenous PS promotes fusion between TF228 cells expressing X4-tropic Env and TZM-bl cells. Fusion was assayed with the fusion per target cell assay described in

Methods with a modification: GFP-expressing TF228 were added to the monolayer of RFP-expressing TZM-bl. Contacting cells were pretreated with 1 μM TAK-779 or 1 μM AMD-3100 or neither at 22°C. Then exogenous PS was applied and the temperature was immediately raised to 37°C. Fusion was scored as number of co-labeled cells. Fusion extents were normalized to those observed for the untreated cells. For PS-treated cells and for the cells that were not treated with PS fusion was inhibited by AMD-3100 but not by TAK-779. All results are means± SD (*n*=4). Levels of significance of the PS promotion (control + PS vs. control) and AMD-3100 inhibition (control vs. control+AMD-3100) are P<0.001. **B.** Application of exogenous PS promotes fusion between GFP-expressing Env-cells cells and JC10 cells expressing RFP, CD4 and biologically relevant low amounts of CCR5 coreceptor. We analyzed fusion using the fusion per target cell assay. The cells were treated with 1μM TAK-779 (bars 3 and 4), or with 1μM AMD3100 (bars 5 and 6), or with neither (1,2). (Bars 2, 4 and 6) the cells were treated with PS. All results are means± SD (n=4). The level of significance of the PS promotion (bar 2 vs. bar 1) is P<0.001. C, D. CD4 and CCR5 expression in the CD4- and CCR5-expressing HeLa-derived cells with modified TMEM16F expression. **C.** Flow cytometry characterization of CD4 and CCR5 expression in the cells used in the experiments on TMEM16F-dependence of virus-induced PS exposure, Env-mediated fusion and infection (Figures 1C, 3D, 6D). Anti-CD4-BV650 and anti-CCR5 –PeCy7 antibodies were used to stain and analyze control HeLa45 cells (1); HeLa45 cells expressing TMEM1616F shRNA (2); constitutively active mutant TMEM16F (3), TMEM16F-silencing shRNA together with an shRNA-resistant form of the TMEM16F protein (4), two different clones (wt16F, clones 4 and 9) of HeLa45 cells expressing w.t. TMEM16F (5 and 6, respectively) and TZM-bl cells expressing very high levels of CD4 and CCR5 (7). For each cell type we analyzed ~20,000 cells. **D.** A moderate variation in the levels of expression of CD4 and CCR5 between different subclones of HeLa45 cells expressing wt TMEM16F (clones 4 and 9) did not result in a significant variation in the extents of fusion between these cells and Env cells. All results are means± SEM (*n*=3). NS – stands for 'no significant difference'. **E.** The PS-dependent stage in Env-mediated cell-cell fusion precedes the LPC-arrested fusion stage. LPC was applied to co-plated Env-cells and TZM-bl cells immediately prior to raising the temperature to 37°C and removed 1 h later. Neither exogenous PS (4) nor LactC2 (5) had an effect on fusion, when applied at the time of LPC removal. (1) Control without LPC for the untreated cells. (2) LPC was applied and not removed. (3) LPC was applied and removed 1h later. (4,5) LPC was removed in the presence of exogenous PS (4) or 12 μM LactC2 (5). Fusion extents measured with the fusion-per-contact assay described in Methods were normalized to those with untreated cells

(bar 1). All results are means± SEM ($n \geq 3$). The fusion extents presented in Bars 1, 4, 5 and 6 were not statistically different.

Figure S5. A01 has no virucidal activity (A), PS effects on VSV G-mediated fusion (B) and on infection with HIV-1 pseudovirus bearing JR-CSF Env (C,D), related to Figures 5 (A,B) and 6 (C,D). A. To evaluate virucidal activity of A01, pseudoviruses were immobilized on poly-L-lysine coated 96-well black clear bottom plates and pre-treated with varied doses of CaCCinh-A01 or left untreated for 30 min, at 37^0C, 5%CO_2. Following three washes, viruses were overlaid with non-enzymatically detached TZM-bl cells and incubated for 2 h at 37^oC to allow fusion. C52L (1 μM), control for fusion. Data are means ± S.D. of two independent triplicate experiments. **B.** VSV G-mediated cell-cell fusion is promoted by application of exogenous PS and inhibited by blocking cell surface PS with LactC2. Fusion between DEIR PIV cells expressing VSV G and RFP and TZMbl cells expressing GFP was triggered by a 2-min application of acidic media of pH 5.5, 6.0, and 6.2; or, in the control, pH 7.4 medium. Immediately prior to acidic pH application, the cells were treated at 22C° with either exogenous PS or with LactC2 or with neither (green, yellow and blue bars, respectively). After low pH application, the cells were returned to pH 7.4 and, after 30min incubation at 37C°, fusion was detected as appearance of yellow cells (i.e., cells labeled with both RFP and GFP). Fusion extents were quantified by normalizing the number of fused DEIR PIVRFP/TZMbl –GFP cells to the total number of contacts between DER PIV cells and TZMbl cells in the same field of view and presented as means + S.D. (n=4). **C,D.** Single round infection of U87.CD4.CCR5 cells with HIV-1 pseudovirus bearing JR-CSF Env depends on PS externalization in the target cells. Virus was applied at MOI of ~0.5 (6 ng p24/ml; 10^4 cells in 100 μl). **C.** The effects of the blocking accessible PS with LactC2. **D.** The effects of A01 pretreatment of U87.CD4.CCR5 cells. The average numbers of infected cells per field of view at 72h post-infection were normalized to those in the control experiment with neither LactC2 (**A**) nor A01 (**B**) applied. All results are means± SEM (n=4).

Figure S6. Control experiments to verify that TMEM16F expression does not change virus–cell surface binding (A) and that measured A01 effects on infection are not affected by using tdTomato fluorescence reporter (B), related to Figure 6 and to the STAR Methods section. A. Variation of TMEM16F expression and activity in HeLa-derived cells does not substantially change virus–cell surface attachment. The cells were incubated with the GAG-Ruby virions pseudotyped with JR-FL Env (38 ng p24/ml, 10^4 cells in 100 μl) at 22ºC for 45 min in the full

medium. After washing out unbound viral particles, the cells were imaged. Virus binding was quantified as cell-surface associated fluorescence in each field of view. (1) Control HeLa45 (HeLa cells expressing CD4 & CCR5); (2) HeLa45 cells treated with A01 (60μM); (3) HeLa45 cells expressing TMEM16F shRNA; (4) HeLa45 cells expressing wt hTMEM16F; (5) HeLa45 cells expressing the constitutively active mutant of hTMEM16F. All results are means± SD (n>7). **B.** The effects of A01 pretreatment of U87.CD4.CCR5 cells on single round infection with JR-CSF HIV-1 pseudovirus quantified using different fluorescent reporters. The average numbers of infected cells per field of view at 72h post-infection were normalized to those in the control experiments with no A01 applied: 600/well and 2280/well for tandem dimer of Tomato (tdTomato) and PNL4.3-Clover, respectively. All results are means± SD. *n*=4 and n=2 for td Tomato and PNL4.3-Clover, respectively.

Figure S7. Gating strategy used for the flow cytometry analysis of $HIV_{LAI.04}$ infection in the JkT-CCR5 **-derived cells, related to Figure 7 and to the STAR Methods section.** (**A**). Single cells were selected by gating FSC-A vs FSC-H (**B**). (**C**) Live vs dead cells were determined with the LIVE/DEAD Fixable Blue Dead Cell Stain Kit. (**D**) Cells were further analyzed for intracellular p24 gag expression.

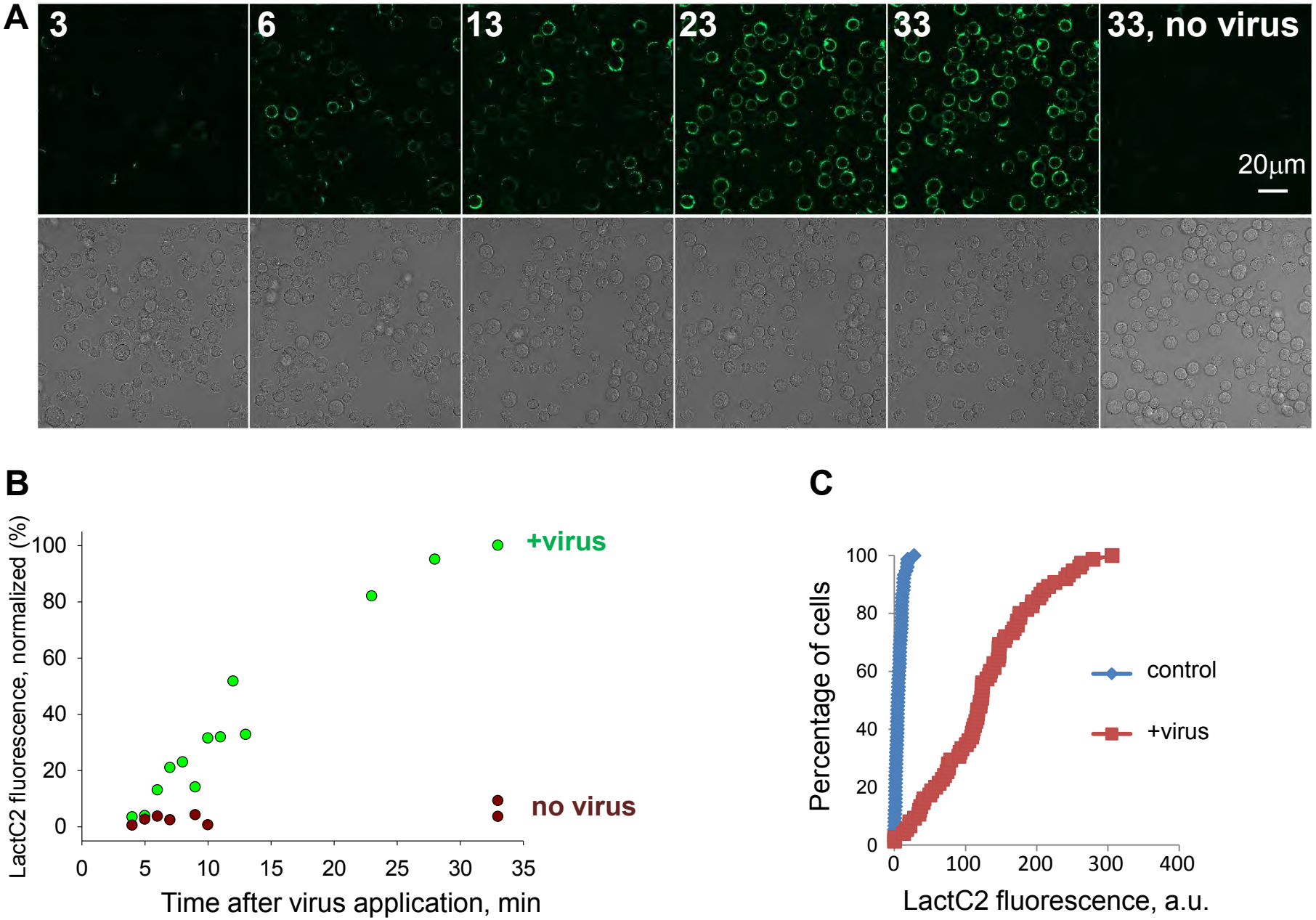
A
3
6
13
23
33
33, no virus
20μm
B
LactC2 fluorescence, normalized (%)
100
80
60
40
20
0
0
5
10
15
20
25
30
35
Time after virus application, min
+virus
no virus
C
Percentage of cells
100
80
60
40
20
0
0
100
200
300
400
LactC2 fluorescence, a.u.
control
+virus

Figure S1

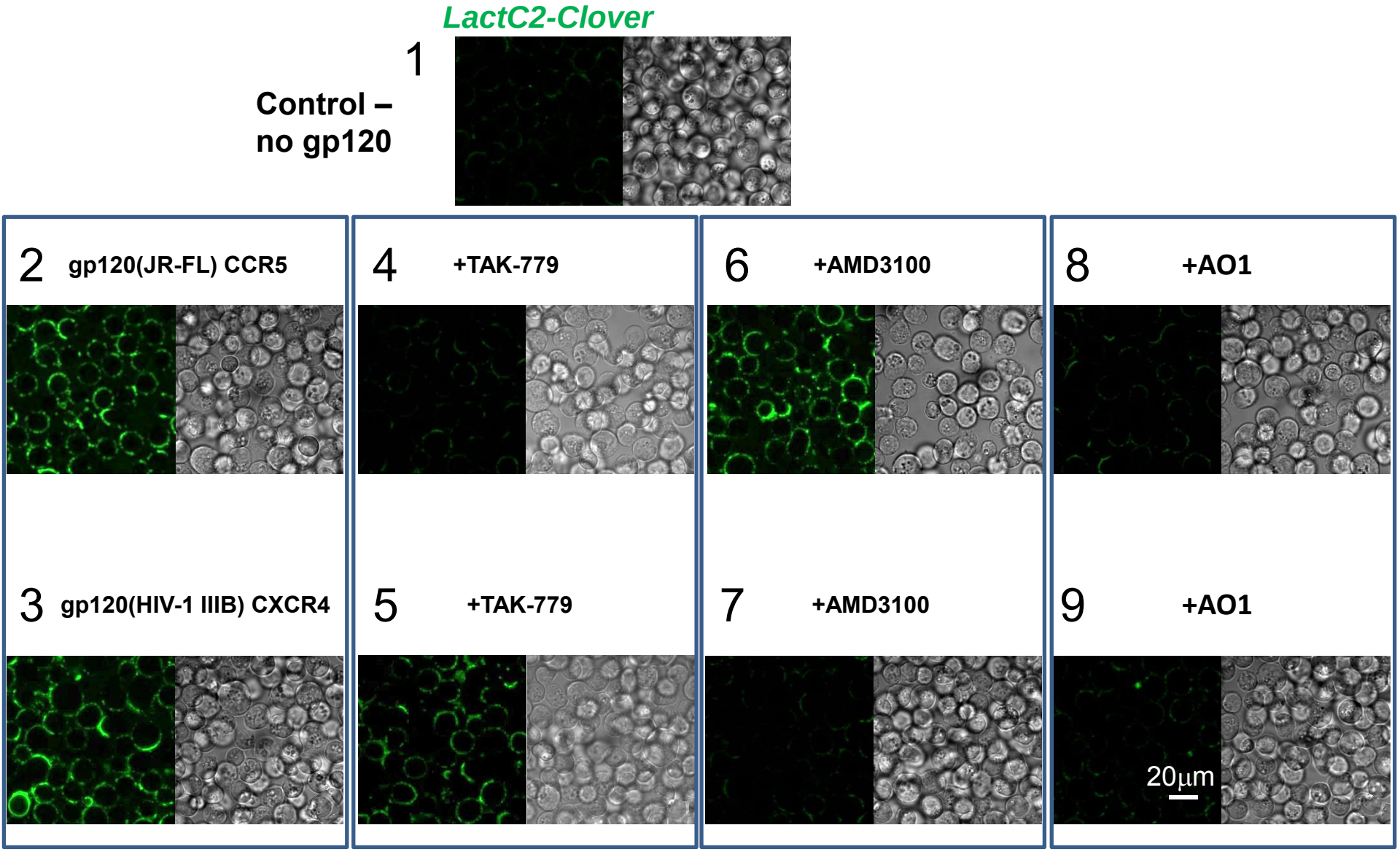
LactC2-Clover
1
Control –
no gp120
2 gp120(JR-FL) CCR5
3 gp120(HIV-1 IIIB) CXCR4
4 +TAK-779
5 +TAK-779
6 +AMD3100
7 +AMD3100
8 +AO1
9 +AO1
20μm

Figure S2

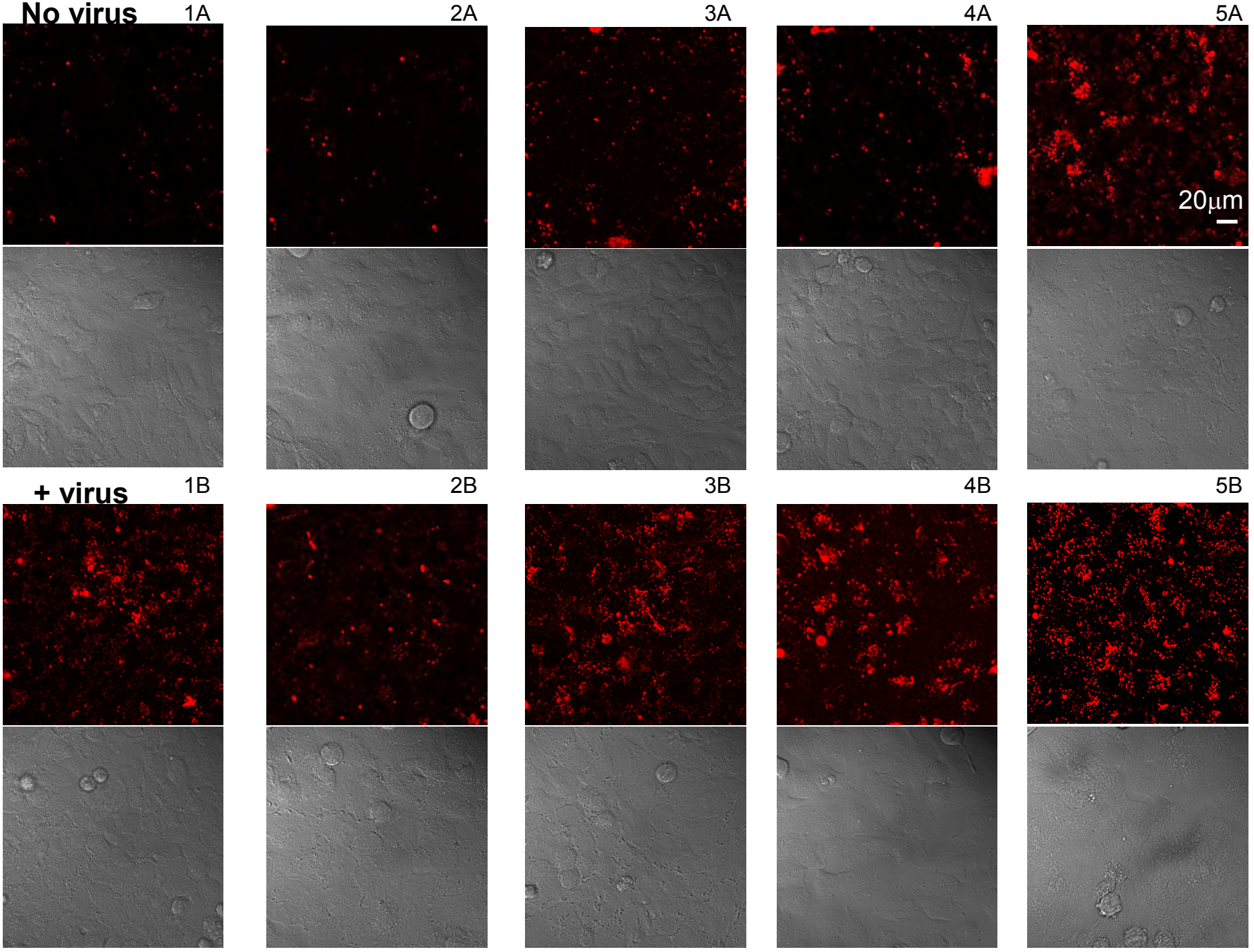

Figure S3

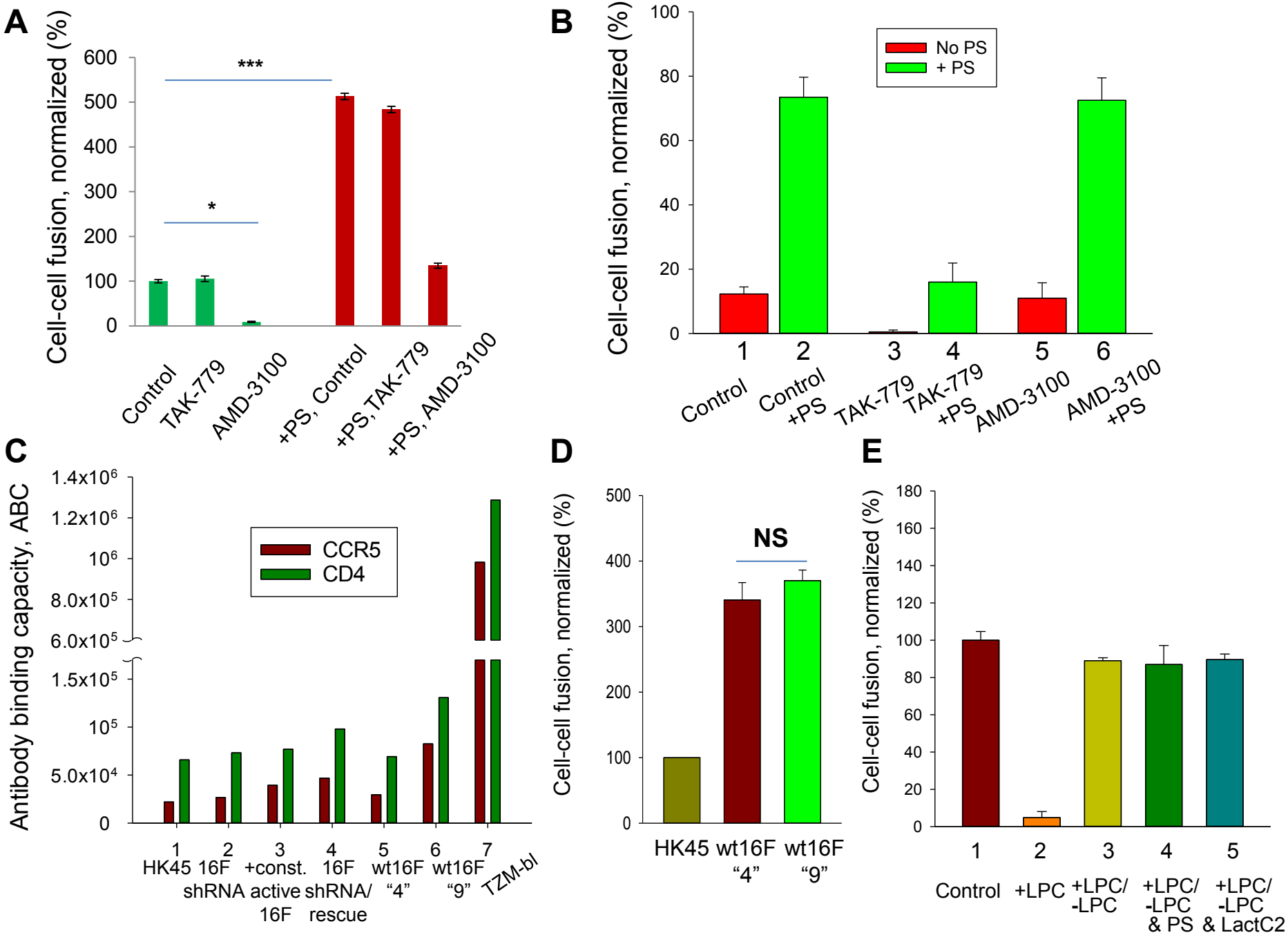
A
Cell-cell fusion, normalized (%)
600
500
400
300
200
100
0
***
*
Control
TAK-779
AMD-3100
+PS, Control
+PS,TAK-779
+PS, AMD-3100
B
Cell-cell fusion, normalized (%)
100
80
60
40
20
0
No PS
+ PS
1
2
3
4
5
6
Control
Control +PS
TAK-779
TAK-779 +PS
AMD-3100
AMD-3100 +PS
C
Antibody binding capacity, ABC
1.4x10⁶
1.2x10⁶
10⁶
8.0x10⁵
6.0x10⁵
1.5x10⁵
10⁵
5.0x10⁴
0
CCR5
CD4
1 HK45
2 16F
3 +const. shRNA active 16F
4 16F shRNA/ rescue
5 wt16F "4"
6 wt16F "9"
7 TZM-bl
D
Cell-cell fusion, normalized (%)
500
400
300
200
100
0
NS
HK45
wt16F "4"
wt16F "9"
E
Cell-cell fusion, normalized (%)
180
160
140
120
100
80
60
40
20
0
1 Control
2 +LPC
3 +LPC/ -LPC
4 +LPC/ -LPC & PS
5 +LPC/ -LPC & LactC2

Figure S4

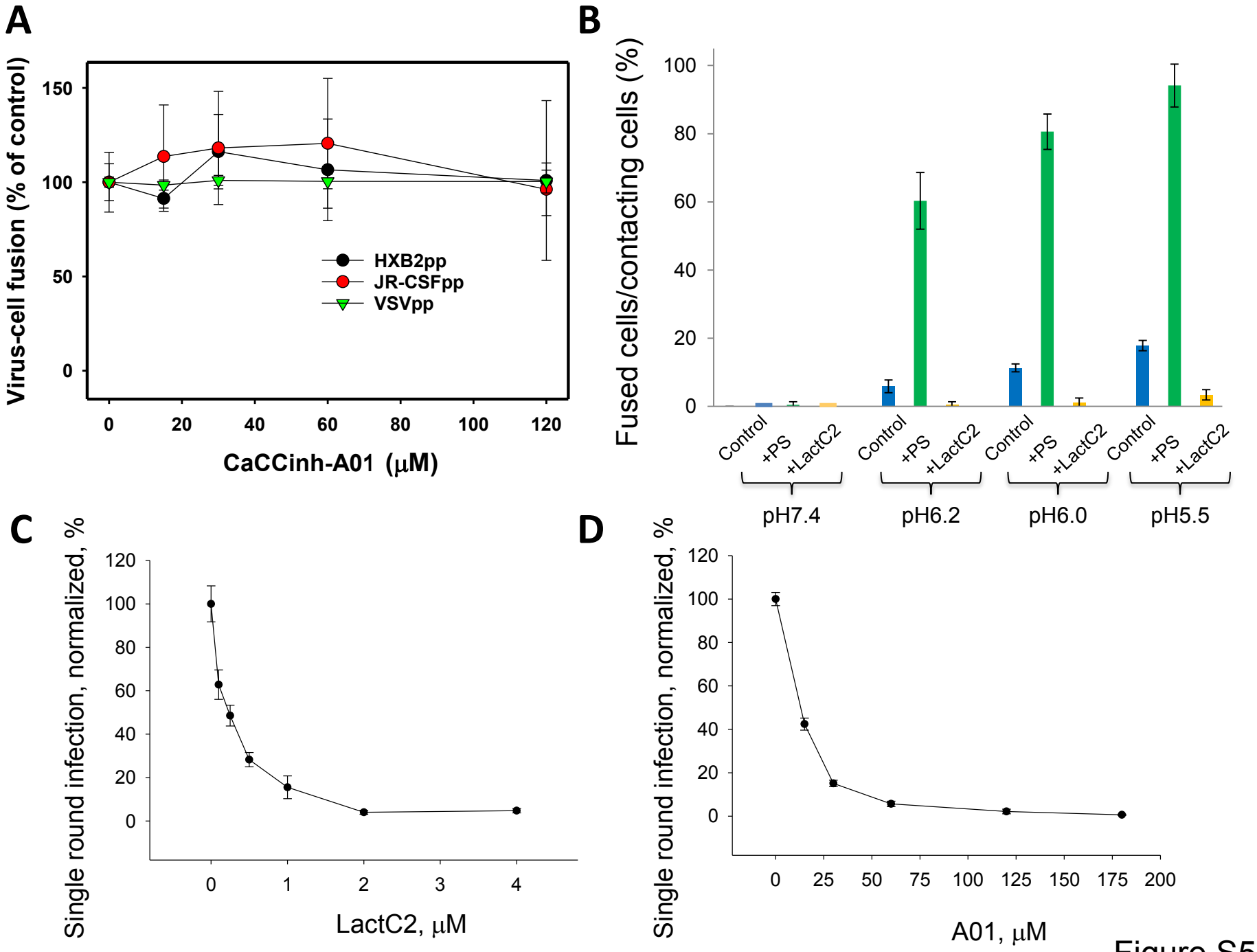
A
Virus-cell fusion (% of control)
150
100
50
0
0
20
40
60
80
100
120
CaCCinh-A01 (μM)
HXB2pp
JR-CSFpp
VSVpp
B
Fused cells/contacting cells (%)
100
80
60
40
20
0
Control
+PS
+LactC2
pH7.4
pH6.2
pH6.0
pH5.5
C
Single round infection, normalized, %
120
100
80
60
40
20
0
0
1
2
3
4
LactC2, μM
D
Single round infection, normalized, %
120
100
80
60
40
20
0
0
25
50
75
100
125
150
175
200
A01, μM

Figure S5

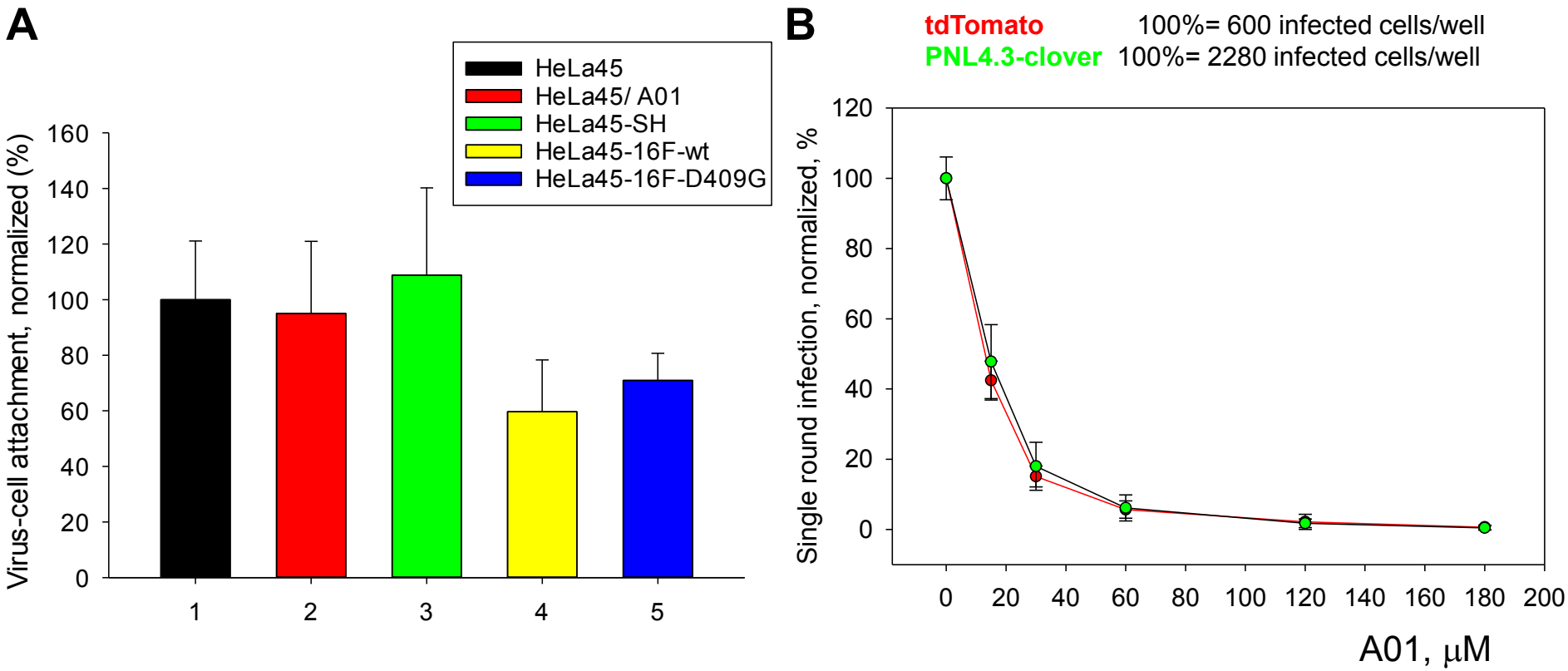
A
HeLa45
HeLa45/ A01
HeLa45-SH
HeLa45-16F-wt
HeLa45-16F-D409G
Virus-cell attachment, normalized (%)
0
20
40
60
80
100
120
140
160
1
2
3
4
5
B
tdTomato 100%= 600 infected cells/well
PNL4.3-clover 100%= 2280 infected cells/well
Single round infection, normalized, %
0
20
40
60
80
100
120
0
20
40
60
80
100
120
140
160
180
200
A01, μM

Figure S6

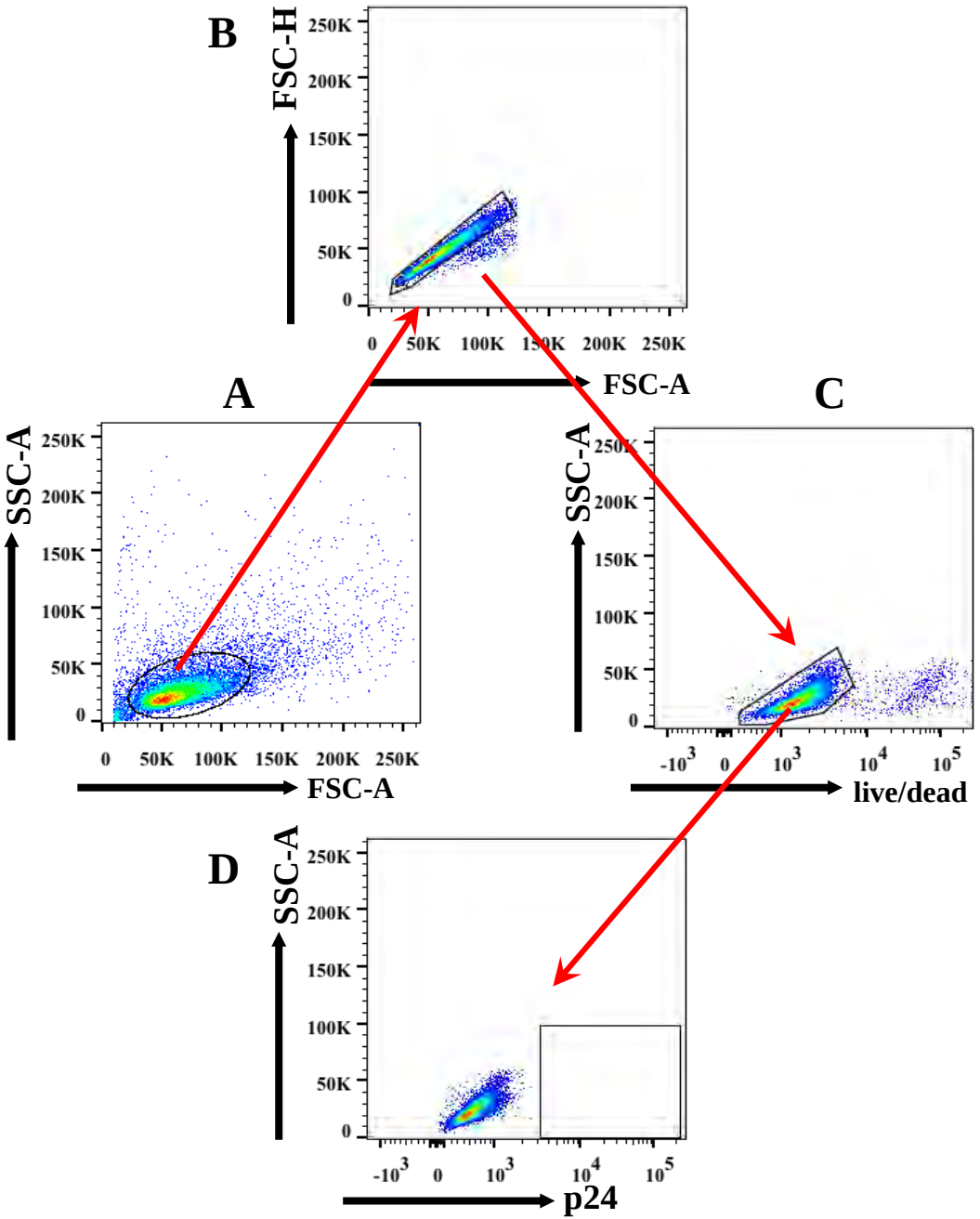
B
FSC-H
250K
200K
150K
100K
50K
0
0 50K 100K 150K 200K 250K
FSC-A
A
SSC-A
250K
200K
150K
100K
50K
0
0 50K 100K 150K 200K 250K
FSC-A
C
SSC-A
250K
200K
150K
100K
50K
0
-10^3 0 10^3 10^4 10^5
live/dead
D
SSC-A
250K
200K
150K
100K
50K
0
-10^3 0 10^3 10^4 10^5
p24

Figure S7